

IDIOPATHIC PULMONARY FIBROSIS

Interleukin-11 is a therapeutic target in idiopathic pulmonary fibrosis

Benjamin Ng^{1,2*}, Jinrui Dong^{2*}, Giuseppe D'Agostino^{2*}, Sivakumar Viswanathan², Anissa A. Widjaja², Wei-Wen Lim^{1,2}, Nicole S. J. Ko², Jessie Tan^{1,2}, Sonia P. Chothani², Benjamin Huang², Chen Xie¹, Chee Jian Pua¹, Ann-Marie Chacko², Nuno Guimarães-Camboa^{3,4,5}, Sylvia M. Evans^{5,6,7}, Adam J. Byrne⁸, Toby M. Maher^{8,9}, Jiurong Liang^{10,11}, Dianhua Jiang^{10,11}, Paul W. Noble^{10,11}, Sebastian Schafer^{1,2†}, Stuart A. Cook^{1,2,12,13†‡}

Copyright © 2019
The Authors, some
rights reserved;
exclusive licensee
American Association
for the Advancement
of Science. No claim
to original U.S.
Government Works

Idiopathic pulmonary fibrosis (IPF) is a progressive fibrotic lung disease where invasive pulmonary myofibroblasts secrete collagen and destroy lung integrity. Here, we show that interleukin-11 (*IL11*) is up-regulated in the lung of patients with IPF, associated with disease severity, and IL-11 is secreted from IPF fibroblasts. *In vitro*, IL-11 stimulates lung fibroblasts to become invasive actin alpha 2, smooth muscle–positive (ACTA2⁺), collagen-secreting myofibroblasts in an extracellular signal-regulated kinase (ERK)-dependent, posttranscriptional manner. In mice, fibroblast-specific transgenic expression or administration of murine IL-11 induces lung myofibroblasts and causes lung fibrosis. IL-11 receptor subunit alpha-1 (*Il11ra1*)-deleted mice, whose lung fibroblasts are unresponsive to profibrotic stimulation, are protected from fibrosis in the bleomycin mouse model of pulmonary fibrosis. We generated an IL-11-neutralizing antibody that blocks lung fibroblast activation downstream of multiple stimuli and reverses myofibroblast activation. In therapeutic studies, anti-IL-11 treatment diminished lung inflammation and reversed lung fibrosis while inhibiting ERK and SMAD activation in mice. These data prioritize IL-11 as a drug target for lung fibrosis and IPF.

INTRODUCTION

Idiopathic pulmonary fibrosis (IPF) is a fibrotic lung disease characterized by epithelial injury and chronic activation of invasive fibroblasts that deposit and remodel the extracellular matrix (ECM) (1, 2). Aging, genetic, and environmental factors are known to trigger IPF, but the mechanisms underlying disease pathology remain poorly understood (2). Anti-inflammatory agents do not improve clinical outcomes (3), and fibroblast biology is of central importance in IPF (4). Antifibrotic small-molecule drugs such as nintedanib (5) and pirfenidone (6) are approved for the treatment of IPF but have notable toxicities (2). Despite best medical practice, IPF remains a progressive disease and an unmet clinical need. Unfortunately, several recent clinical trials of potential new IPF therapies have not shown efficacy, and new approaches are needed (7).

Transforming growth factor-β (TGFβ) family proteins are considered the principal profibrotic cytokines and may play a role in lung fibrosis (8). However, direct or indirect targeting of TGFβ

activation has major side effects, including lung fibrosis itself (9–11), due to the pleiotropic roles of TGFβ family members. We previously screened for fibroblast-specific mediators of TGFβ1 activity in human cardiac fibroblasts and identified a crucial role of interleukin-11 (IL-11) in cardiovascular fibrosis. Fibroblast-to-myofibroblast transition in the heart and kidney was found to be dependent on an autocrine IL-11 signaling loop, and IL-11 receptor subunit alpha-1 (*Il11ra1*)-deleted mice were protected from both cardiac and renal fibrosis, despite previous reports that IL-11 is a cardioprotective and anti-fibrotic cytokine (12).

Although our studies of the heart and kidney highlighted the importance of pathogenic IL-11 signaling in cardiovascular fibroblast biology, the role of this cytokine for fibro-inflammatory disorders in other organs is mostly unexplored. *IL11* is one of the most up-regulated genes in pulmonary fibroblasts from patients suffering from scleroderma-associated interstitial lung disease or IPF (13), but there are few studies on IL-11 function in the lung. Conflicting data suggest that IL-11 can either cause lung inflammation and airway obstruction (14) or protect from lung inflammation and damage in murine models of hyperoxia or endotoxin-induced lung injury (15–17). Likely because of these discrepancies, the study of IL-11 biology in the lung has progressed little. In multiple recent and detailed reviews of lung fibrosis and IPF, there is no mention of IL-11, further emphasizing the lack of knowledge on IL-11 in lung fibrosis (2, 7, 18).

Here, we first explored whether *IL-11* up-regulation in human lung is a robust feature of IPF and whether *IL11* expression is linked with IPF fibroblast pathobiology or clinical features of IPF severity. We then examined whether IL-11 signaling inhibits or promotes lung fibrosis through its activity in lung fibroblasts to address the discrepancies in the published literature. We ended by developing a therapeutic strategy to block IL-11 signaling that we tested in a mouse model of pulmonary fibrosis, which might be translated to patients with IPF.

¹National Heart Centre Singapore, 169609 Singapore, Singapore. ²Duke–National University of Singapore Medical School, 169857 Singapore, Singapore. ³Institute for Cardiovascular Regeneration, Goethe University Frankfurt, Frankfurt 60590, Germany. ⁴German Center for Cardiovascular Research DZHK, Berlin 10785, Germany. ⁵Skaggs School of Pharmacy and Pharmaceutical Sciences, University of California, San Diego, La Jolla, CA 92093, USA. ⁶Department of Medicine, University of California, San Diego, La Jolla, CA 92093, USA. ⁷Department of Pharmacology, University of California, San Diego, La Jolla, CA 92093, USA. ⁸Fibrosis Research Group, Inflammation, Repair and Development Section, National Heart and Lung Institute, Imperial College, London SW7 2AZ, UK. ⁹NIHR Biomedical Research Unit, Royal Brompton Hospital, London SW7 2AZ, UK. ¹⁰Department of Medicine, Cedars-Sinai Medical Center, Los Angeles, CA 90048, USA. ¹¹Women's Guild Lung Institute, Cedars-Sinai Medical Center, Los Angeles, CA 90048, USA. ¹²National Heart and Lung Institute, Imperial College, London SW3 6LY, UK. ¹³MRC-London Institute of Medical Sciences, Hammersmith Hospital Campus, London W12 0NN, UK.

*These authors contributed equally to this work.

†These authors jointly directed this work.

‡Corresponding author. Email: stuart.cook@duke-nus.edu.sg

RESULTS**IL-11 is up-regulated and associated with disease severity in IPF**

IPF is a heterogeneous disease with variable rates of progression predicted by the severity of lung pathophysiology, notably diffusing capacity of the lung for carbon monoxide (DL_{CO}) (% predicted), as well as radiographic and histological features of fibrosis severity (19). Bauer *et al.* (20) assessed physiological lung parameters and, in parallel, profiled global pulmonary gene expression using RNA microarrays. To explore *IL11* expression in the context of IPF, we reanalyzed this large lung dataset (see Materials and Methods) of patients with IPF ($n = 122$) and controls ($n = 92$).

IL11 was significantly up-regulated in the IPF lung [false discovery rate (FDR) = 7.16×10^{-9}] (Fig. 1A and tables S1 and S2 in data file S1). We then built linear regression models and tested for correlation between RNA expression and functional parameters to investigate the relationship between lung *IL11* expression, lung function, and fibrosis. After adjusting for age and sex, we found a strong negative correlation between pulmonary *IL11* RNA expression and lung function parameters such as DL_{CO} ($P = 1.28 \times 10^{-7}$), forced expiratory volume (FEV; $P = 2.07 \times 10^{-3}$), and forced vital capacity (FVC; $P = 5.64 \times 10^{-4}$) in patients with IPF (Fig. 1, B and C), but not in healthy individuals (fig. S1, A and B, and tables S3 and S4 in data file S1). This suggests that *IL11* expression is particularly high in patients who suffer from more severe forms of IPF where lung function is markedly reduced. In addition, *IL11* RNA was positively correlated with fibrosis marker RNA such as *COL1A1* ($P = 2.28 \times 10^{-4}$) and *TIMP1* ($P = 4.52 \times 10^{-7}$) in the lungs of patients with IPF (Fig. 1D, fig. S1C, and tables S5 and S6 in data file S1). Both findings suggest that increased IL-11 signaling in IPF is associated with reduced pulmonary function and an enhanced fibrotic response. In contrast to these findings, other IL-6 family members implicated in IPF [Oncostatin M (OSM) and *IL6*], as well as *IL13* that was unsuccessfully targeted in IPF clinical trials (21), were all down-regulated in IPF lungs and not associated with fibrosis gene expression (Fig. 1D and fig. S1D). These RNA expression patterns in human disease suggest a preeminent role for IL-11 in fibrotic lung conditions, especially when compared to other signaling molecules.

These data are supported by a study from 2013 where *IL-11* was shown to be the most highly up-regulated gene in fibrotic lung disease fibroblasts (13). Reanalysis of an additional study (22) revealed that *IL11* was highly expressed in invasive IPF fibroblasts (Fig. 1E) when compared to noninvasive IPF fibroblasts ($P = 3.91 \times 10^{-3}$). To investigate IL-11 at the protein level, we performed enzyme-linked immunosorbent assays (ELISAs) on culture supernatants of primary lung fibroblasts from patients with IPF and found that IPF cells secrete greater amounts of IL-11 than control fibroblasts both at baseline ($P = 3.56 \times 10^{-3}$) and in response to TGF β 1 stimulation (5 ng ml $^{-1}$, 24 hours; $P = 6.18 \times 10^{-4}$) (Fig. 1F). We performed immunostaining for IL-11 and actin alpha 2, smooth muscle (ACTA2), a marker of myofibroblasts, in lung sections from control individuals and patients with IPF. IL-11 protein was hardly detectable in control lung tissue but markedly elevated in IPF lung samples ($P = 8.27 \times 10^{-3}$) along with ACTA2, although accurate colocalization is challenging because IL-11 is a secreted protein (Fig. 1G and fig. S2).

IL-11 is a profibrotic cytokine in the lung

To test experimentally whether IL-11 is pro- or antifibrotic in the lung, we first incubated primary human pulmonary fibroblasts with recombinant human IL-11 (rhIL-11) (5 ng ml $^{-1}$, 24 hours). IL-11

induced noncanonical extracellular signal-regulated kinase (ERK) signaling, ACTA2 expression ($P = 1.11 \times 10^{-16}$), and collagen secretion ($P = 1.90 \times 10^{-2}$) as measured by high-content imaging, Western blotting, and collagen assays, although to a lesser extent than TGF β 1 (Fig. 2, A and B, and fig. S3, A to C). Induction of the fibrotic response by IL-11 was ERK dependent and can be blocked with ERK inhibitors U0126 ($P < 2.2 \times 10^{-16}$) and PD98059 ($P = 1.11 \times 10^{-16}$) in primary lung fibroblasts as measured by quantification of ACTA2 and collagen type I alpha 1 chain (COL1A1) immunostaining (Fig. 2C and fig. S3D). Fibroblast invasion, critical in the pathobiology of IPF, was also triggered by IL-11 (20 ng ml $^{-1}$; $P = 4.58 \times 10^{-6}$) (Fig. 2D). We also performed RNA sequencing (RNA-seq) of IL-11 and TGF β 1-stimulated lung fibroblasts (5 ng ml $^{-1}$, 24 hours). Transforming and plotting the data into log ratio (M) and mean average (A) scales in an MA plot showed negligible changes in global transcription after IL-11 stimulation, especially when compared to TGF β 1. Together with the apparent ERK-dependent increase in profibrotic protein expression at the same time point (Fig. 2C), this is consistent with a posttranscriptional effect of noncanonical IL-11 signaling in pulmonary fibroblasts, similar to our previous finding in cardiac fibroblasts (12). Similar to the effect of rhIL-11 on human cells, recombinant mouse IL-11 on primary mouse lung fibroblasts also induced fibrogenic protein expression such as ACTA2 ($P = 2.91 \times 10^{-13}$) or collagen ($P = 4.07 \times 10^{-3}$) and triggered cell migration ($P = 3.58 \times 10^{-3}$) and invasion ($P = 9.75 \times 10^{-4}$) (fig. S3, G to J). This demonstrates a conserved profibrotic effect of IL-11 on lung fibroblasts across species and underlines the relevance of modeling IL-11 effects in the mouse lung.

To examine IL-11-dependent regulation of ECM production in vivo, we administered daily subcutaneous injections of recombinant mouse IL-11 (100 $\mu\text{g kg}^{-1}$) into transgenic mice that express green fluorescent protein (GFP) under the control of a *Col1a1* promoter (referred to as *Col1a1-GFP* mice) (23) and analyzed the lungs after 21 days. Fluorescent imaging showed that IL-11 induced *Col1a1* $^+$ fibroblast accumulation throughout the lung parenchyma ($P = 9.21 \times 10^{-3}$) (Fig. 2E and fig. S4A). Administration of IL-11 increased lung weights ($P = 2.40 \times 10^{-4}$) and pulmonary collagen content (~32%; $P = 3.10 \times 10^{-3}$) and induced fibrogenic gene expression (fig. S4, B to D). IL-11 has previously been shown to induce cardiac, kidney, and liver fibrosis, suggesting a consistent effect of IL-11 on fibroblast activation across mouse tissues (12, 24).

To further investigate the potential fibrogenic role of IL-11, we modeled the specific overexpression of *Il11* in fibroblasts in vivo. We previously generated transgenic mice in which mouse *Il11* was knocked into the *Rosa26* locus under the control of *loxP-Stop-loxP* sites to enable cell type-specific, Cre recombinase-mediated transgene induction (12). We crossed these mice with mice that express tamoxifen-inducible Cre recombinase driven by the mouse collagen type I alpha 2 (*Col1a2*) promoter to specifically drive *Il11* expression in *Col1a2* $^+$ fibroblasts in an inducible manner (referred to as *Il11-Tg* mice) (12). After 3 weeks of fibroblast-specific *Il11* overexpression, we observed collagen deposition in peribronchial and peribronchiolar areas, thickening of the alveolar septae, and widespread interstitial fibrosis in the lungs, which was confirmed using histopathological scoring ($P = 1.14 \times 10^{-4}$) (Fig. 2F and fig. S4E). Lung collagen content was significantly increased (~25%; $P = 7.43 \times 10^{-3}$) along with up-regulation of fibrosis-related genes and ECM proteins (Fig. 2, G and H, and fig. S4, F and G). Lung fibroblasts from *Il11-Tg* mice secreted large amounts of IL-11 and were highly invasive in transwell Matrigel invasion assays ($P = 2.18 \times 10^{-3}$), which is a prominent feature of pulmonary IPF fibroblasts (4, 22) (Fig. 2I and fig. S4H).

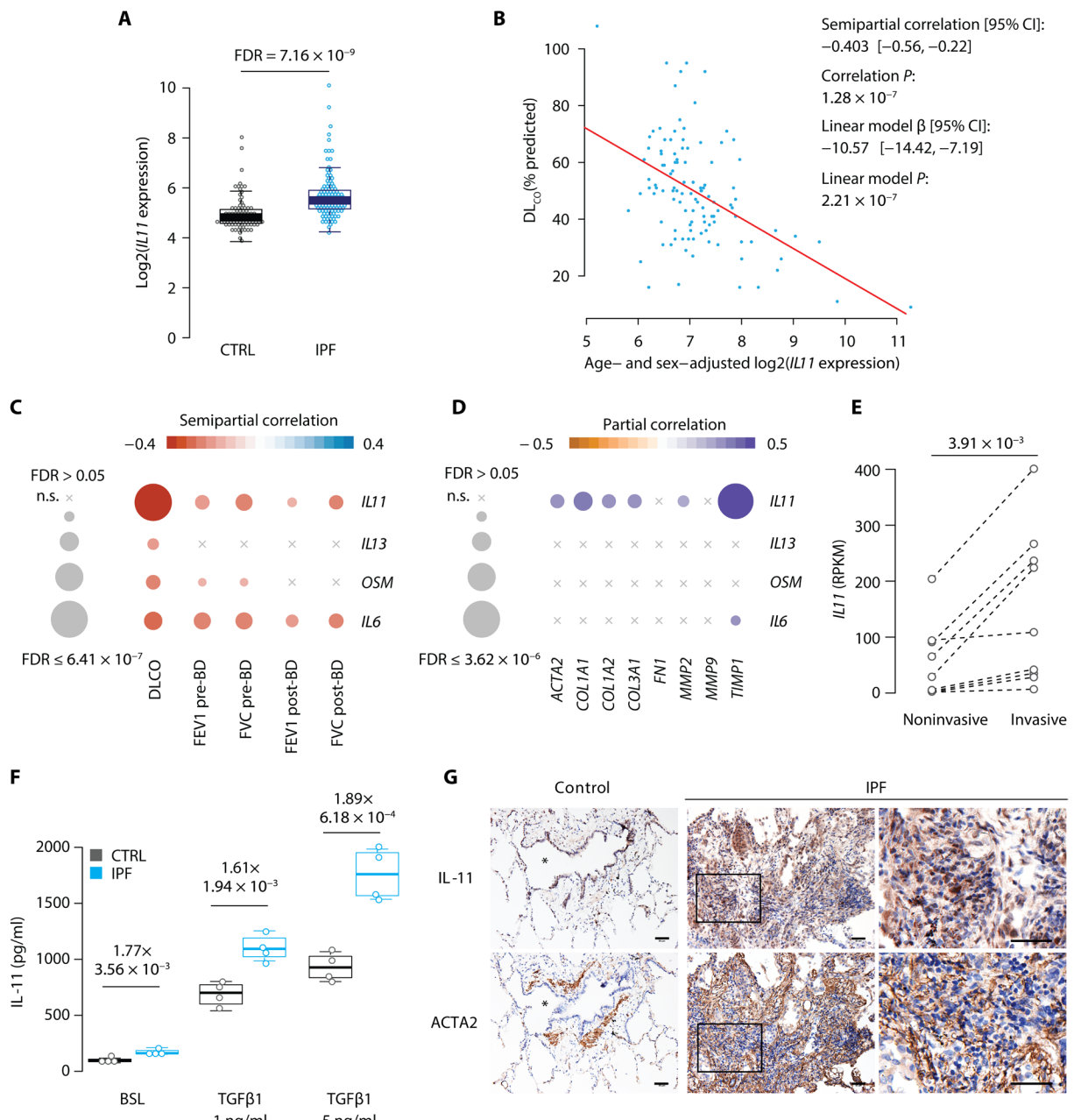


Fig. 1. IL-11 is up-regulated in IPF lung and fibroblasts. (A) Log-transformed normalized gene expression values in lung tissue from patients with IPF ($n = 122$) and controls ($n = 92$), with differential expression FDR-adjusted P value. (B) Linear relationship and association between lung function, measured as DL_{CO} % predicted and log of age- and sex-adjusted IL11 expression ($n = 110$). (C) Semipartial Spearman correlation of IL-6 family cytokines (IL11, IL6, and OSM) and IL13 with lung function. n.s., nonsignificant. (D) Partial Spearman correlation of IL-6 family cytokines (IL11, IL6, and OSM) and IL13 with fibrosis-associated genes. Correlation P values were adjusted for FDR for each cytokine separately. Colors (from red to blue or orange to purple) indicate Spearman's correlation coefficient, from negative to positive values. Dot sizes are proportional to $-\log_{10}(\text{adjusted } P \text{ value})$: the larger the dot, the lower the FDR value. X denotes nonsignificant values (FDR > 0.05). (E) Expression of IL11 in noninvasive and invasive lung fibroblasts from patients with IPF by RNA-seq analysis ($n = 9$). (F) Secreted quantities of IL-11 from primary lung fibroblasts from control (healthy donor) and patients with IPF treated with TGF β 1 (0, 1, or 5 ng ml $^{-1}$, 24 hours; $n = 4$). (G) Representative images of IL-11 and ACTA2 immunostaining in serial sections of lung tissue from a patient with IPF and healthy controls ($n = 3$). Bronchiolar regions are demarcated with an asterisk in control sections. The boxed regions are shown at higher magnification in the right panels. Scale bars, 50 μm . Data in (A) to (D) were derived from Gene Expression Omnibus (GEO) datasets GSE47460. Data in (E) were derived from GSE11893. Data in (A) and (F) are represented as median \pm interquartile range (IQR), and whiskers represent IQR \times 1.5. Adjusted P values for each comparison are shown above black lines. P values in (E) and (F) were determined by Student's t tests. FEV1, forced expiratory volume 1; BD, bronchodilation; BSL, baseline.

IL-11 is required for lung fibroblast activation

To evaluate whether IL-11 signaling is involved in other well-studied profibrotic pathways, we stimulated primary human lung fibroblasts

with recombinant TGF β 1 and performed RNA-seq. IL11 was one of the most highly up-regulated transcripts genome-wide (fold change = 31.15, $P = 4.13 \times 10^{-97}$) (Fig. 3A and table S7 in data file S1).

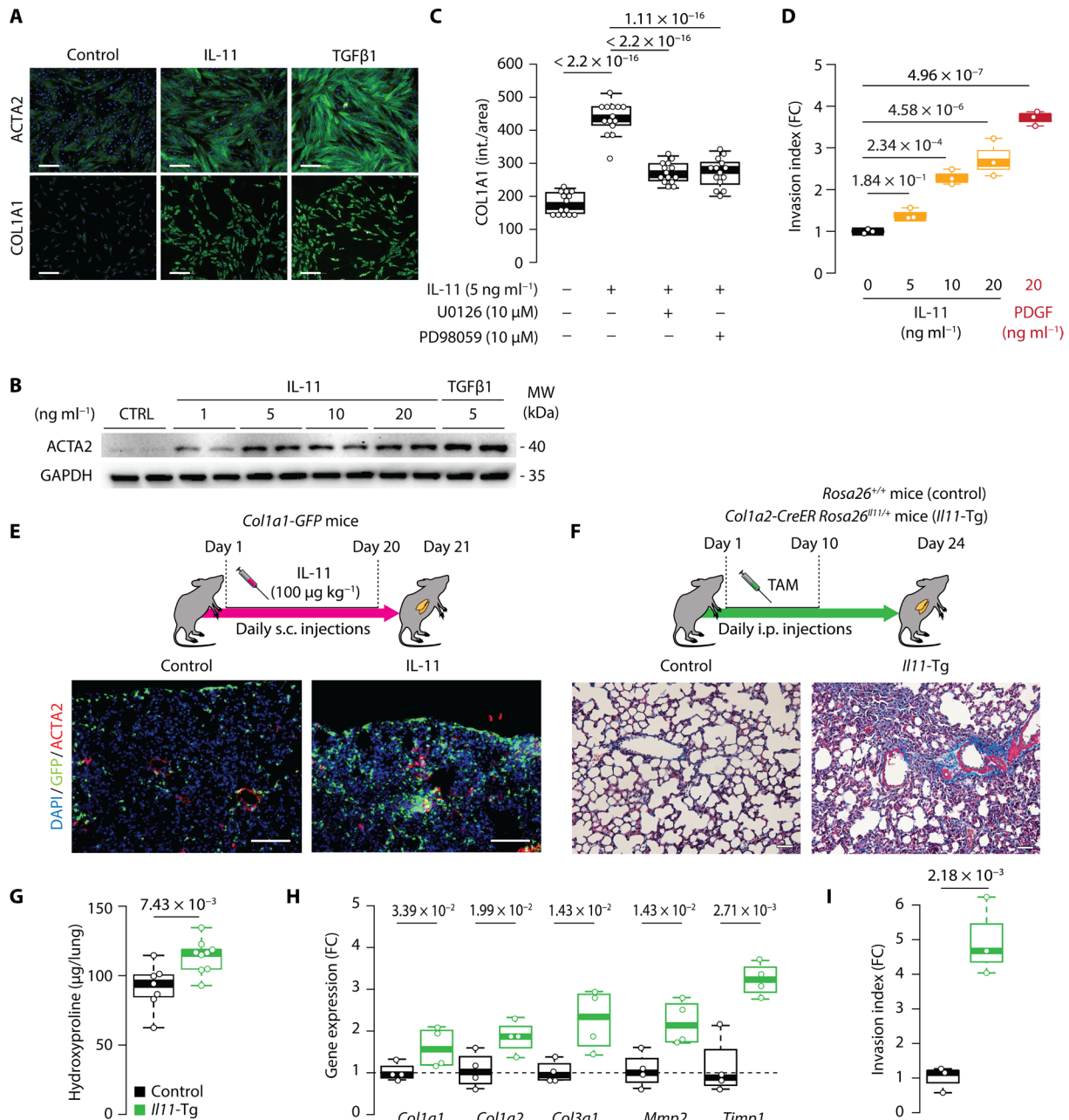


Fig. 2. IL-11 activates pulmonary fibroblasts and induces lung fibrosis. (A) Representative images of ACTA2 or COL1A1 immunostaining in primary human lung fibroblasts treated with IL-11 or TGF β 1 (5 ng ml $^{-1}$, 24 hours; n = 3). Cells were counterstained with 4',6-diamidino-2-phenylindole (DAPI) to visualize nuclei. Scale bars, 200 μ m. Quantitative data are shown in fig. S3A. (B) Western blot of ACTA2 expression in lung fibroblasts treated with increasing dose of IL-11 (1–20 ng ml $^{-1}$, 24 hours) or TGF β 1 (5 ng ml $^{-1}$, 24 hours) (n = 2). Glyceraldehyde-3-phosphate dehydrogenase (GAPDH) was used as a loading control. CI, confidence interval; MW, molecular weight. (C) Quantification of COL1A1 immunostaining in primary human lung fibroblasts treated with IL-11 (5 ng ml $^{-1}$, 24 hours) in the presence of MEK inhibitors U0126 or PD98059. One representative dataset from three independent biological experiments is shown (14 measurements per condition per experiment). (D) Matrigel invasion indices of primary human lung fibroblasts induced by IL-11 or PDGF (n = 3). (E) Schematic and representative fluorescence images of GFP-positive cells in lung tissue of *Col1a1-GFP* mice treated with daily subcutaneous (s.c.) injections of mouse IL-11 (100 μ g kg $^{-1}$) as compared to saline-injected controls. Sections were immunostained for ACTA2 to visualize pulmonary smooth muscle cells and myofibroblasts and counterstained with DAPI to visualize nuclei. Scale bars, 100 μ m. (n = 4). (F) Schematic strategy for the inducible expression of *Il11* in *Col1a2*-expressing cells in mice (*Il11-Tg*) (top) and representative Masson's trichrome staining of lung sections from *Il11-Tg* and littermate control mice (bottom). Scale bars, 50 μ m. TAM, tamoxifen; i.p., intraperitoneal. (G) Lung hydroxyproline content (n = 7 control and n = 9 *Il11-Tg*) and (H) mRNA expression of fibrosis genes in *Il11-Tg* and littermate control mice lungs (n = 4). (I) The spontaneous Matrigel-invading capacity of lung fibroblasts isolated from *Il11-Tg* and control mice was determined (n = 3). Data represented as median \pm IQR, and whiskers represent IQR \times 1.5. P values were determined by Student's t test and were corrected for FDR using the Benjamini-Hochberg method in (H). FC, fold change.

In addition to TGF β 1, we also stimulated pulmonary fibroblasts with other fibrogenic factors that are actively under investigation by the scientific community as therapeutic targets for IPF: fibroblast growth factor 2 (FGF2), platelet-derived growth factor (PDGF), OSM, IL-13, and endothelin 1 (EDN1) (25–29). ELISA measurements of IL-11 in the supernatant showed that all factors tested significantly induced IL-11 secretion from primary lung fibroblasts (Fig. 3B), which suggests activation of IL-11 signaling downstream of diverse profibrotic stimuli.

To test whether IL-11 signaling was important downstream of these profibrotic cytokines, we isolated lung fibroblasts from *I11ra1*^{-/-} mice and stimulated them with these factors. When applied to *I11ra1*^{-/-} fibroblasts, TGF β 1 did not promote myofibroblast differentiation or ECM production as monitored by high-content imaging of COL1A1 expression and by Sirius red-based quantification of secreted collagen (Fig. 3, C and D, and fig. S5A). Matrigel invasion and transwell migration assays indicated reduced invasive capacity ($P = 3.84 \times 10^{-3}$) and migration ($P = 1.31 \times 10^{-4}$) of *I11ra1*^{-/-} fibroblasts when compared to *I11ra1*^{+/+} fibroblasts after TGF β 1 stimulation (Fig. 3, E and F). Complementing these genetic knockout experiments, small interfering RNA-mediated knockdown of either *I11* ($P = 2.19 \times 10^{-11}$) or *I11ra1* ($P = 4.97 \times 10^{-12}$) confirmed a reduction in actin alpha 2, smooth muscle-positive (ACTA2 $^+$) cells after TGF β 1 stimulation (fig. S5B).

To determine whether the antifibrotic effects of IL-11 inhibition were related to the loss of TGF β responsiveness, we treated *I11ra1*^{-/-} and *I11ra1*^{+/+} fibroblasts with TGF β 1 (5 ng ml $^{-1}$, 24 hours) and performed Western blot analysis. Although the fibrogenic activity of TGF β 1 was greatly reduced in *I11ra1*^{-/-} lung fibroblasts (Fig. 3, C to F), SMAD phosphorylation was preserved, indicating intact canonical TGF β signaling in the context of IL-11 inhibition (fig. S5C). In keeping with this, TGF β 1 treatment resulted in very similar RNA expression changes in both *I11ra1*^{-/-} or *I11ra1*^{+/+} fibroblasts: RNA-seq revealed nearly identical fold changes of SMAD/TGF β 1 target genes in both cell types after stimulation (fig. S5D and table S8 in data file S1). These results show that deletion of *I11ra1* does not impair the TGF β -induced transcriptional response in vitro and suggests that the prevention of fibroblast activation occurs downstream of TGF β -driven SMAD activation at the posttranscriptional level.

Next, to determine whether the fibrogenic properties of other IL-11-inducing cytokines (PDGF, FGF2, OSM, IL-13, and EDN1) were dependent on IL-11 signaling, we treated *I11ra1*^{-/-} and wild-type fibroblasts with these factors and monitored for fibroblast activation by ACTA2, COL1A1 immunostaining, and collagen assays. Similar to our data for TGF β 1, *I11ra1*^{-/-} lung fibroblasts did not transform into ACTA2 $^+$ myofibroblasts or express COL1A1 after stimulation with any of the additional profibrotic factors we tested (Fig. 3, G and H, and fig. S5, E to G). As such, IL-11 signaling appears to be a nonredundant mechanism required for the transformation of lung fibroblasts to myofibroblasts downstream of a variety of fibrogenic stimuli.

Bleomycin-induced pulmonary fibrosis is attenuated in *I11ra1*^{-/-} mice

To determine the role of IL-11 in lung fibrosis in vivo, we used the established bleomycin (BLM) model of murine pulmonary fibrosis (30, 31). Wild-type mice were subjected to a single dose of BLM, and lung homogenates were collected on days 7, 14, and 21, which coincides with the early fibrogenic phase (day 7) and fibrotic phase (days 14 to 21) of this model (Fig. 4A). IL-11 was significantly

up-regulated in the lung during the late fibrogenic phase 14 days after BLM treatment ($P = 3.69 \times 10^{-2}$) and most highly expressed during the peak of fibrosis at day 21 ($P = 1.00 \times 10^{-7}$) (Fig. 4B and fig. S6A). This was concurrent with the up-regulation of collagen, type III, alpha 1 (COL3A1) ($P = 3.48 \times 10^{-2}$), and fibronectin ($P = 1.14 \times 10^{-3}$) at day 14, with peak expression of both ECM proteins at day 21 (COL3A1: $P = 1.03 \times 10^{-3}$; fibronectin: $P = 1.53 \times 10^{-6}$) (Fig. 4B and fig. S6A). We profiled canonical [signal transducer and activator of transcription 3 (STAT3)] and noncanonical (ERK) IL-11 signaling pathways during the time course and found that ERK activation followed a similar pattern to IL-11 up-regulation and was most prominent at day 21 ($P = 1.05 \times 10^{-6}$), whereas STAT3 appeared maximally phosphorylated at earlier time points and peaked by day 14 ($P = 2.36 \times 10^{-3}$) (Fig. 4C and fig. S6B).

We administered BLM to *I11ra1*^{-/-} mice to examine the role of IL-11 in the progression of lung fibrosis (Fig. 4D). Histological assessment of the lungs demonstrated abundant collagen deposition and profound architectural disruption in wild-type mice 21 days after BLM treatment, whereas these pathologies were significantly reduced in *I11ra1*^{-/-} mice ($P = 9.10 \times 10^{-3}$) (Fig. 4E and fig. S6, C to E). Collagen content of the lung was also lower, as indicated by a significantly reduced hydroxyproline content (~48%; $P = 1.30 \times 10^{-3}$) (Fig. 4F). The reduction of ECM deposition in the lungs of *I11ra1*^{-/-} mice was confirmed using Western blotting of COL3A1 and fibronectin (Fig. 4G and fig. S6F). However, there was no effect of the *I11ra1* deletion on mortality after BLM (fig. S6G). To further investigate the impact of the genetic deletion of *I11ra1* on downstream signaling pathways in lung fibrosis, we performed Western blotting of phosphorylated ERK, STAT3, and SMAD using lung homogenates from *I11ra1*^{-/-} and wild-type mice 21 days after BLM. Deletion of *I11ra1* significantly reduced the activation of ERK ($P = 6.53 \times 10^{-4}$), STAT3 ($P = 3.33 \times 10^{-4}$), and, to a lesser extent, SMAD signaling pathways ($P = 1.32 \times 10^{-2}$) (Fig. 4H and fig. S6H). However, because of potential secondary changes in cell composition or cytokine expression in vivo, it is not clear which of these effects are directly or indirectly driven by IL-11. Nonetheless, together with the histological and protein expression data, these results indicate that *I11ra1*^{-/-} mice are protected from BLM-induced lung fibrosis.

Development of a neutralizing anti-IL-11 antibody

Encouraged by our findings, we next investigated whether IL-11 in the lung can be targeted therapeutically by developing and applying antibodies that bind to and neutralize IL-11. Mice were immunized with human IL-11, and after specific reactivity was confirmed, antibody-producing cells were isolated and fused with mouse myeloma cells and subcloned to generate monoclonal hybridoma cell lines. IL-11 was then expressed on the surface of human embryonic kidney cells, and using a fluorescent-activated cell sorting-based approach, candidate antibody pools with specific IL-11 binding were prioritized (fig. S7, A and B; see also Materials and Methods). In vitro fibrosis screens identified several clones that blocked both mouse and human fibroblast activation downstream of TGF β 1 by neutralizing the IL-11 autocrine signaling loop (fig. S7C). Affinity measurements based on surface plasmon resonance technology indicated that the clone X203 had equilibrium dissociation constants for mouse and human IL-11 of 2.38 and 4.14 nM, respectively (fig. S7, D and E).

The efficacy of X203 in cellular assays that quantify fibroblast activation by measuring the secretion of fibrosis marker proteins (MMP2 and TIMP1) ranged from 3.4 to 27.2 ng ml $^{-1}$ half maximal

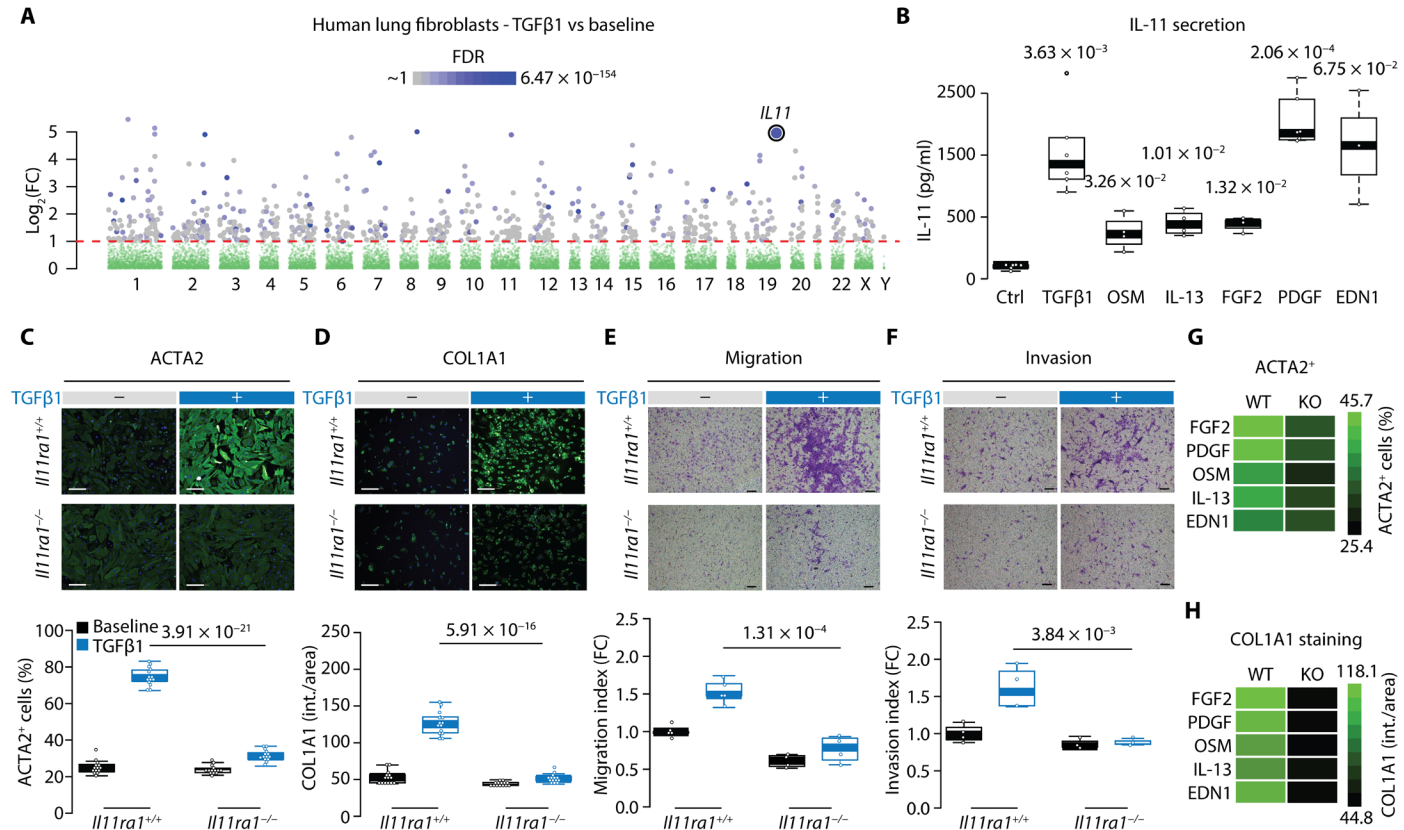


Fig. 3. IL-11 signaling is required for pulmonary fibroblast activation. **(A)** Graphical representation of RNA-seq data showing genes up-regulated in human lung fibroblasts after stimulation with TGF β 1 (5 ng ml $^{-1}$, 24 hours) binned by chromosome. Significance values are shown only for genes with log 2 (fold change) > 1 (red dashed line). **(B)** ELISA of secreted IL-11 from mouse lung fibroblasts after 24-hour treatment with TGF β 1 (5 ng ml $^{-1}$), FGF2 (10 ng ml $^{-1}$), PDGF (50 ng ml $^{-1}$), OSM (50 ng ml $^{-1}$), IL-13 (50 ng ml $^{-1}$), or EDN1 (250 ng ml $^{-1}$) ($n = 3$ to 4). **(C and D)** Representative immunofluorescence images (top) and quantification (bottom) of ACTA2⁺ cells and COL1A1 immunostaining of primary lung fibroblasts from *I11ra1*^{+/+} and *I11ra1*^{-/-} mice treated with TGF β 1 (5 ng ml $^{-1}$, 24 hours). One representative dataset from three independent biological experiments is shown (14 measurements per condition per experiment). Scale bars, 200 μ m. **(E and F)** Comparison of TGF β 1-induced migration or Matrigel invasion between primary lung fibroblasts from *I11ra1*^{+/+} and *I11ra1*^{-/-} mice ($n = 4$ to 5). Scale bars, 150 μ m. **(G and H)** Heatmaps showing the immunofluorescence quantification of ACTA2⁺ cells and COL1A1 immunostaining (intensity/area) in *I11ra1*^{+/+} [wild type (WT)] and *I11ra1*^{-/-} [knockout (KO)] lung fibroblasts treated as depicted in (B). Quantitative data are shown in fig. S5. Data in (B) to (F) are represented as median \pm IQR, and whiskers represent IQR \times 1.5. All comparisons were analyzed by Student's *t* test; *P* values in (B) were corrected using the Benjamini-Hochberg procedure.

inhibitory concentration (IC₅₀) (fig. S7, F to H). The inhibition of fibrogenic protein production by X203 was subsequently confirmed in TGF β 1-treated lung fibroblasts. High-content imaging-based analysis demonstrated that X203 treatment significantly reduced TGF β 1-induced ACTA2 and COL1A1 expression ($P = 6.73 \times 10^{-11}$ and $P = 7.65 \times 10^{-12}$, respectively), along with a marked decrease in Sirius red-based quantification of collagen secretion ($P = 1.47 \times 10^{-3}$) (Fig. 5A and fig. S8, A to C). Similar to the genetic deletion of *I11ra1*, neutralization of IL-11 with X203 also resulted in a reduction of TGF β 1-driven fibroblast invasion ($P = 9.04 \times 10^{-6}$) and migration ($P = 8.33 \times 10^{-4}$), as assessed by transwell and Matrigel assays (fig. S8, D and E). Western blotting confirmed that X203 inhibited IL-11-dependent ERK phosphorylation but had no effect on STAT3 activation, which remained elevated (Fig. 5B and fig. S8F).

Consistent with data from *I11ra1*-deleted pulmonary fibroblasts (Fig. 3), X203 blocked fibrogenic protein production by pulmonary fibroblasts downstream of additional profibrotic factors (FGF2, PDGF, OSM, IL-13, and EDN1) by neutralizing endogenous IL-11 in a range of fibrosis assays, including imaging-based quantification of ACTA2⁺ cells and Sirius red assay-based quantification of secreted

collagen (Fig. 5, C to E, and fig. S8, G to I). The profibrotic effects of these factors were associated with IL-11-induced ERK activation, and Western blotting confirmed this dependency (fig. S8J).

To examine the therapeutic potential of X203, we investigated the utility of X203 to inhibit the profibrotic phenotypes of primary lung fibroblasts from patients with IPF. We found that X203 markedly inhibited TGF β 1-induced ACTA2⁺ fibroblast-to-myofibroblast transition ($P = 1.28 \times 10^{-13}$) and COL1A1 expression ($P = 2.16 \times 10^{-4}$) in IPF fibroblasts (fig. S9). Furthermore, X203 treatment significantly reduced the Matrigel invasive capacity of patient-derived fibroblasts ($P = 1.09 \times 10^{-2}$) (Fig. 5F). Although preventing fibrosis progression is important, reversal of established fibrosis is of greater therapeutic value. To evaluate whether X203 was capable of reversing the fibrotic response in vitro, we pretreated lung fibroblasts with TGF β 1 for 24 hours to induce fibroblast-to-myofibroblast transformation. The cells were then incubated with media containing either X203 or IgG antibody for an additional 24 hours. High-content imaging-based analysis of ACTA2 and COL1A1 expression, along with Sirius red-based quantification of secreted collagen, revealed that X203 significantly reversed the profibrotic cellular phenotypes of TGF β 1-transformed

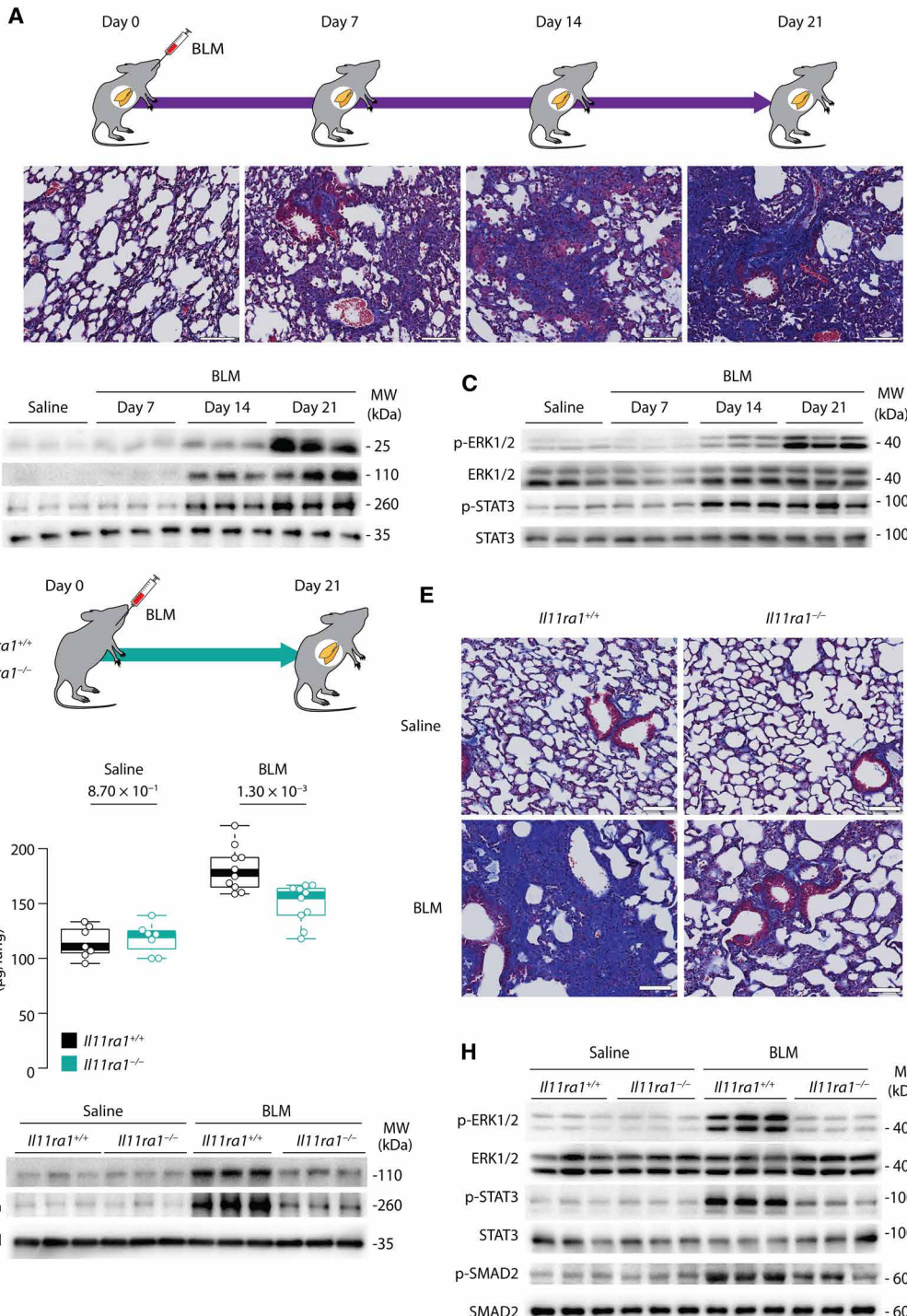


Fig. 4. Bleomycin-induced pulmonary fibrosis is attenuated in *IL1ra1*-null mice. (A) Schematic showing the induction of pulmonary fibrosis and the progressive accumulation of lung collagen visualized by Masson's trichrome staining after BLM challenge. A single dose of BLM was administered oropharyngeally, and lung tissues were collected at the indicated time points. (B) Western blot of IL-11, COL3A1, and fibronectin and (C) expression of ERK and STAT3 and their phosphorylated isoforms in lung homogenates of BLM-challenged mice ($n = 3$ per time point). (D) Schematic showing the induction of pulmonary fibrosis in *IL1ra1*^{+/+} and *IL1ra1*^{-/-} mice. (E) Masson's trichrome staining of lung sections and (F) lung hydroxyproline content of *IL1ra1*^{+/+} and *IL1ra1*^{-/-} mice 21 days after BLM ($n = 4$ to 5 per saline group and $n = 10$ per BLM group). Scale bars, 100 μ m. (G) Western blot of COL3A1 and fibronectin and (H) expression of phosphorylated and total ERK, STAT3, and SMAD2 in lung homogenates of BLM-challenged *IL1ra1*^{+/+} and *IL1ra1*^{-/-} mice ($n = 3$). GAPDH was used as a loading control. Quantification data for Western blots are shown in fig. S6. Data in (F) are represented as median \pm IQR, and whiskers represent IQR \times 1.5. *P* values were determined by Student's *t* test.

Downloaded from <http://stm.scienmag.org/> at Umeå University on September 28, 2019

myofibroblasts within 24 hours of antibody treatment (ACTA2⁺: $P = 1.31 \times 10^{-14}$; COL1A1: $P = 7.05 \times 10^{-5}$; secreted collagen: $P = 6.40 \times 10^{-4}$) (Fig. 5, G and H).

Therapeutic targeting of IL-11 prevents and reverses pulmonary fibrosis

To determine whether X203 is effective as an antifibrotic *in vivo* by neutralizing IL-11 activity in the lung, we performed preclinical studies in the BLM model for pulmonary fibrosis. Pharmacokinetics and

biodistribution of X203 were measured with intravenously injected radiolabeled X203 (^{125}I -X203; $4.2 \mu\text{Ci}/2.5 \mu\text{g}/100 \mu\text{l}$) in the lungs of wild-type C56BL/6 mice. More than 5% of ^{125}I -X203 was present in the lung 24 hours after injection, and the antibody half-life in blood was about 9 days (fig. S10, A and B). We then investigated the potential of X203 to prevent pulmonary fibrosis using the common interventional time point of 7 days after BLM (31). In dose-finding experiments, we administered X203 at 10 mg kg^{-1} intraperitoneally every 3 days. Although this dose had no effect on lung fibrosis, there was a partial but significant reduction in ERK activation by day 21 after BLM ($P = 5.74 \times 10^{-3}$), showing target engagement but incomplete target coverage (fig. S10, C and D). For all subsequent *in vivo* therapeutic experiments, we used a higher dose of X203 (20 mg kg^{-1}), which we found previously to be effective in treating liver fibrosis (24). When

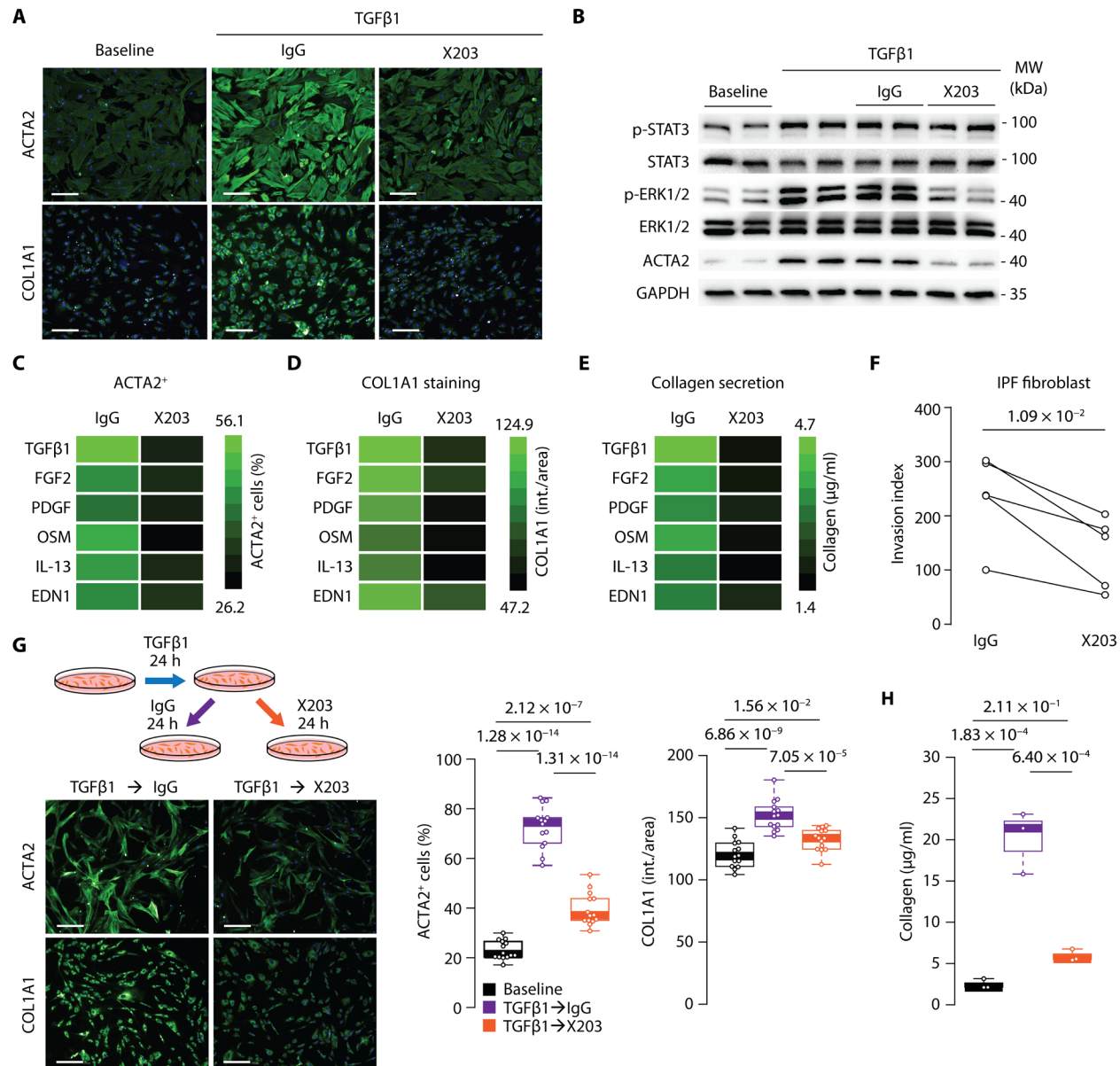


Fig. 5. Neutralizing anti-IL-11 antibodies inhibit and reverse lung fibroblast activation. (A) Representative images of ACTA2 and COL1A1 immunostaining in mouse lung fibroblasts treated with TGF β 1 (5 ng ml^{-1} , 24 hours) in the presence of X203 or immunoglobulin G (IgG) control antibodies ($2 \mu\text{g ml}^{-1}$). Scale bars, $200 \mu\text{m}$. (B) Western blot of phosphorylated and total expression of STAT3 and ERK and ACTA2 in total cell lysates of lung fibroblasts treated with TGF β 1 (5 ng ml^{-1} , 24 hours) and IgG or X203 ($2 \mu\text{g ml}^{-1}$; $n = 2$). GAPDH was used as a loading control. (C to E) Heatmaps showing the immunofluorescence quantification of (C) ACTA2 $^{+}$ cells, (D) COL1A1 immunostaining (intensity/area), and (E) secreted collagen concentrations from mouse lung fibroblasts treated with multiple profibrotic stimuli in the presence of X203 or IgG control antibodies. Quantitative data for Western blot and immunostaining are shown in fig. S8. (F) Matrigel invasion capacity of primary lung fibroblast from patients with IPF treated with X203 or IgG control antibodies ($2 \mu\text{g ml}^{-1}$; $n = 5$). (G) Representative images and quantification of ACTA2 $^{+}$ cells and COL1A1 immunostaining (intensity/area) and (H) collagen secretion of TGF β 1-differentiated human lung fibroblasts (5 ng ml^{-1} , 24-hour pretreatment) treated with X203 or IgG control antibodies ($2 \mu\text{g ml}^{-1}$, 24 hours; $n = 3$). One representative dataset from three independent biological experiments is shown in (G) (14 measurements per condition per experiment). Scale bars, $200 \mu\text{m}$. Data in (G) and (H) are represented as median \pm IQR, and whiskers represent IQR \times 1.5. P values were determined by Student's t test in (F) and one-way ANOVA (Tukey's test) in (G) and (H).

X203 was administered on alternate days at this higher dose from day 7 to 21 after BLM, there was a significant reduction in both lung weights ($P = 1.67 \times 10^{-2}$) and parenchymal disruption by histological assessment ($P = 1.44 \times 10^{-4}$) (Fig. 6, A to C, and fig. S10, E and F). There was no effect on overall survival (fig. S10G). Consistent with the histological data, lung hydroxyproline content was greatly reduced (~55%; $P = 6.86 \times 10^{-4}$) in X203-treated mice (Fig. 6D).

To gain additional insights into the mechanisms by which IL-11 inhibition affected lung fibrosis and disease progression overall, we performed RNA-seq of lungs (Fig. 6A) and found that the expression of ECM-related genes was reduced in X203-treated mice as compared to IgG controls (Fig. 6E and table S9 in data file S1). Western blot analysis of COL3A1 and fibronectin and quantitative reverse transcription polymerase chain reaction analysis of *Col1a1*, *Col1a2*, and

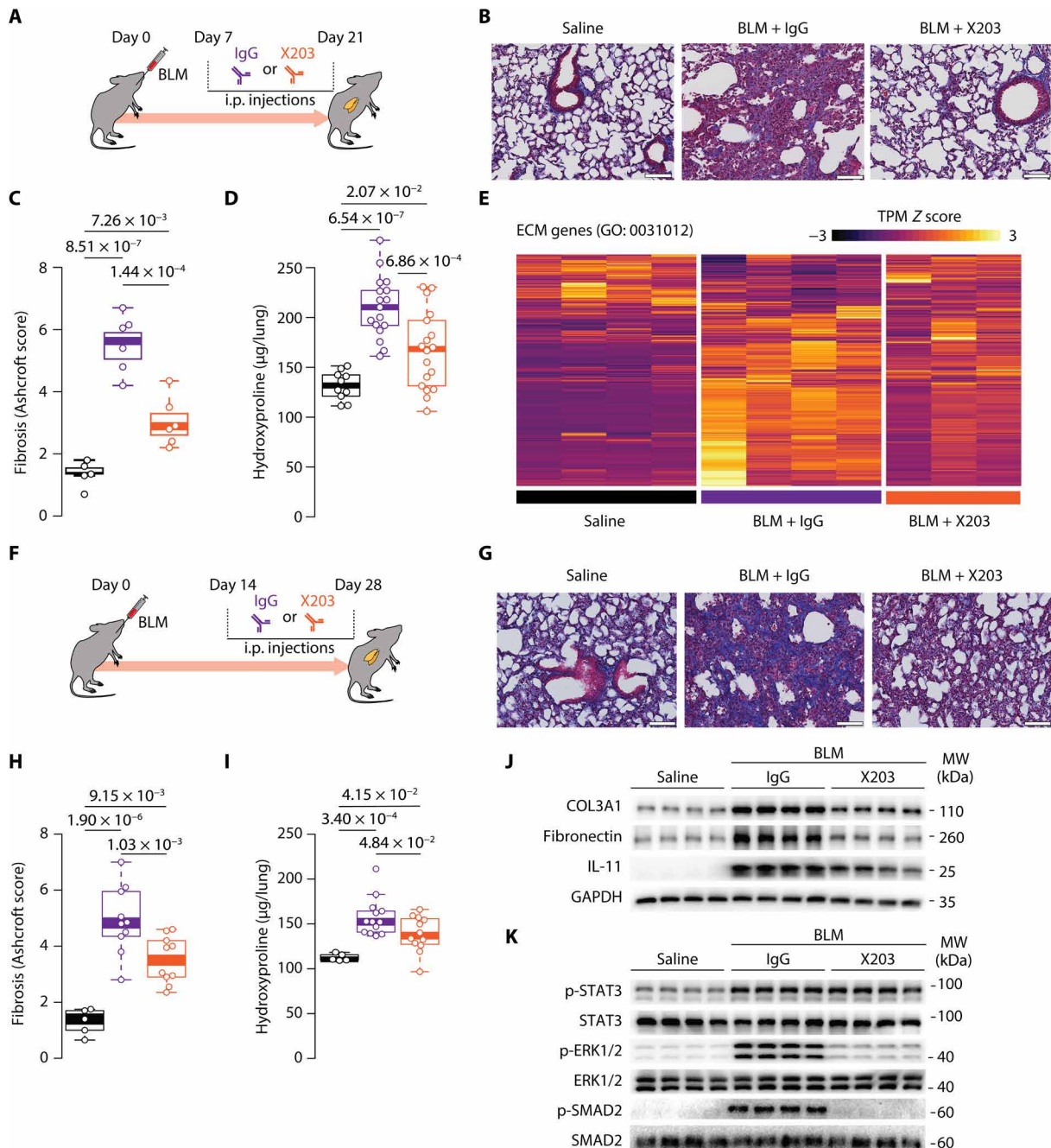


Fig. 6. Neutralizing anti-IL-11 antibodies prevent and reverse pulmonary fibrosis. (A) Schematic showing early therapeutic blockade of IL-11 in the BLM model. X203 (20 mg kg^{-1} , alternate days) was injected intraperitoneally starting at day 7, and lungs were assessed on day 21 after BLM administration. (B) Representative Masson's trichrome staining of lung sections from X203- or IgG-treated mice in the prophylactic lung fibrosis model. Scale bars, $100 \mu\text{m}$. (C) Fibrosis score ($n = 5$ to 6) and (D) lung hydroxyproline content ($n = 10$ to 18) of X203- or IgG-treated mice in the prophylactic lung fibrosis model. (E) Transcript per million (TPM) heatmap showing scaled expression of all ECM genes as classified in the GO category 0031012 (ECM genes) by RNA-seq analysis of lungs from X203- or IgG-treated mice in the prophylactic lung fibrosis model ($n = 3$ to 4). (F) Schematic showing the blockade of IL-11 in the therapeutic lung fibrosis model. Mice were injected with X203 (20 mg kg^{-1} , alternate days) starting at day 14, and lungs were assessed on day 28 after BLM administration. (G) Representative Masson's trichrome staining of lung sections from X203- or IgG-treated mice in the therapeutic lung fibrosis model. Scale bars, $100 \mu\text{m}$. (H) Fibrosis score ($n = 5$ to 10) and (I) hydroxyproline content ($n = 5$ to 13) in the lungs of X203- or IgG-treated mice in the therapeutic lung fibrosis model. (J) Western blots of COL3A1, fibronectin, and IL-11 and (K) phosphorylation and total expression of STAT3, ERK, and SMAD2 in lung homogenates of X203- or IgG-treated mice in the therapeutic lung fibrosis model ($n = 4$). GAPDH was used as a loading control. Quantitative data for Western blots are shown in figs. S12 and S13. Data represented as median \pm IQR, and whiskers represent IQR \times 1.5. P values were determined by one-way ANOVA (Tukey's test).

Col3a1 expression in lung lysates further validated this observation (fig. S10, H to J). In addition, an increase in *Mmp2/Timp1* ratio ($P = 3.71 \times 10^{-2}$), a signature of preferential ECM remodeling (32), was evident in X203-treated mice as compared to controls (fig. S10K). The BLM model has a strong inflammatory component (33), and we used RNA-seq to assess whether anti-IL-11 therapy has anti-inflammatory activity. Gene Set Enrichment Analysis (GSEA) showed a strong effect of X203 on ECM genes ($P = 3.17 \times 10^{-4}$) and also, but to a lesser extent, on genes of the Gene Ontology (GO) category “Inflammatory Response (GO: 0006954),” which was significantly enriched ($P = 3.17 \times 10^{-4}$) (fig. S11 and tables S10 to S12 in data file S1). This suggests a primary role for IL-11 in fibroblasts, which express high amounts of *Il11ra* and a potentially secondary effect on inflammatory cells.

We then determined whether anti-IL-11 therapy could reverse lung fibrosis by treating mice later in the disease course after collagen content has plateaued (from day 14 to 28 after BLM) (Fig. 6F). In the context of later intervention, X203 therapy significantly reduced collagen deposition and parenchymal disruption by histological assessment ($P = 1.03 \times 10^{-3}$), lung weights ($P = 1.48 \times 10^{-3}$), and lung hydroxyproline content (~42% decrease; $P = 4.84 \times 10^{-2}$) but again had no effect on survival as compared to IgG treatment (Fig. 6, G to I, and fig. S12, A to C). Consistent with the histological and biochemical data, later intervention with X203 reduced the expression of ECM proteins COL3A1 ($P = 3.14 \times 10^{-5}$) and fibronectin ($P = 1.89 \times 10^{-5}$), as well as IL-11 levels ($P = 2.18 \times 10^{-3}$) in the lungs 28 days after BLM (Fig. 6J and fig. S12, D to F). These data show that anti-IL-11 therapy promotes resolution of lung fibrosis in mice.

To dissect the signaling pathway(s) important for IL-11–driven lung fibrosis, we profiled the activation status of canonical (STAT3) and noncanonical (ERK) IL-11 signaling and also SMAD signaling pathways by Western blotting of lung homogenates from X203- or IgG-treated mice after either the early (days 7 to 21) or the later (days 14 to 28) interventions. Blocking IL-11 signaling markedly reduced ERK activation *in vivo* (early: $P = 1.01 \times 10^{-2}$; late: $P = 4.57 \times 10^{-8}$), whereas STAT3 phosphorylation remained elevated (Fig. 6K and fig. S13), consistent with our *in vitro* data. Anti-IL-11 therapy also reduced SMAD activation (early: $P = 2.94 \times 10^{-4}$; late: $P = 8.87 \times 10^{-7}$), as seen in the earlier BLM studies in *Il11ra1*-deleted mice.

DISCUSSION

IPF is a progressive disease, associated with pathological accumulation of myofibroblasts that secrete ECM, leading to disruption of lung architecture, pulmonary failure, and, ultimately, death. Here, we show that IL-11 is up-regulated in the lung and fibroblasts from patients with IPF, associated with IPF severity, and that IL-11 drives pulmonary fibroblast activation across species. IL-11 is robustly induced in primary cultures of human and mouse lung fibroblasts by a variety of profibrotic stimuli implicated in IPF. Targeting of IL-11–dependent ERK activation can reverse the myofibroblast phenotype and ameliorate lung fibrosis. We propose that therapeutic inhibition of IL-11, a point of signaling convergence downstream of multiple profibrotic stimuli, might be effective in reducing lung fibrosis in IPF. Furthermore, targeting IL-11 may avoid the toxicities previously associated with inhibiting TGF β isoforms themselves directly or indirectly (9–11, 34).

For the most part, the previously published literature on IL-11 suggests that this cytokine is protective, anti-inflammatory, and

antifibrotic across various organs. In previous studies in mice, rhIL-11 was shown to be cardioprotective and to reduce fibrosis in the heart (35, 36) and to protect the liver from ischemia/reperfusion injury and acetaminophen-induced damage (37, 38). In the kidney, rhIL-11 was found to be protective in mouse models of nephrotoxic nephritis and renal ischemia and reperfusion injury (39, 40). rhIL-11 also protected the bowel from radiation injury or mucosal inflammation in mice (41, 42). In the lung, rhIL-11 was reported to be anti-inflammatory in endotoxin-induced injury in mice (17). On the contrary, Tang *et al.* (14) showed that rhIL-11 causes airway inflammation and subepithelial fibrosis when overexpressed in Club/Clara cells. This was contradicted in a study using the same model that showed strong protective effects of rhIL-11 against hyperoxia-induced mortality (15). However, Chen *et al.* (43) demonstrated that IL-13–induced lung remodeling was dependent on endogenous IL-11 signaling, and Moodley *et al.* showed that IL-11 was mitogenic in lung fibroblasts from both healthy individuals and patients with IPF through sustained stimulation of noncanonical ERK signaling, although its association with fibrosis was not investigated (44). Likely as a result of this contradictory literature, mostly on the basis of data using foreign rhIL-11 in the mouse, there is no mention of IL-11 in recent comprehensive scientific reviews of IPF or lung fibrosis (2, 7, 18).

The results we present here build upon our previous studies of IL-11 in cardiovascular and hepatic fibrosis, which show that IL-11 is an important driver of fibrosis in the heart, kidney, and liver (12, 24). In lung fibroblasts, we show that IL-11 is robustly induced by a variety of profibrotic cytokines relevant to the pathogenesis of lung fibrosis and IPF (including TGF β 1, PDGF, FGF2, IL-13, OSM, and EDN1) and that the inhibition of IL-11 signaling blocks lung fibroblast activation induced by all of these factors via an ERK-dependent mechanism. RNA-seq analysis of IL-11–treated lung fibroblasts showed that IL-11 does not stimulate a transcriptomic response, which provides further evidence that IL-11 acts through a posttranscriptional mechanism, consistent with our previous findings in cardiac fibroblasts (12). Recently, it was shown that *IL-11* underlies human lung fibrosis in Hermansky-Pudlak syndrome (HPS) (45). In this study, *IL-11* was highly expressed in HPS mutant human lung organoids, and deletion of *IL11* prevented fibrosis, which supports the notion that IL-11 is an important driver of lung fibrosis.

In two independent gain-of-function models, either systemic administration or genetic and fibroblast-specific expression, *Il11* was sufficient to drive lung fibrosis *in vivo*. Fibrosis in these models was associated with the up-regulation of key profibrotic genes and accumulation of ECM in the lung within 3 weeks. It is important to highlight key differences in our gain-of-function approaches as compared to previous studies. We administered or overexpressed mouse IL-11 in mice, whereas previous studies were based on the administration or overexpression of alien rhIL-11 in murine systems, which protected against injury or caused airway disease as mentioned above (14, 15, 17). We recently found that rhIL-11 is largely ineffective in activating mouse cardiac fibroblasts and that very high doses of human IL-11 are required to have any activity in murine cells (12). This suggests that the use of human IL-11 in the mouse may result in differential or nonphysiologically relevant effects in the mouse, which requires further study.

We note that after BLM challenge, anti-IL-11 antibody therapy inhibits ERK and SMAD but not STAT3 activation, whereas ERK, SMAD, and STAT3 were inhibited in *Il11ra1*^{−/−} mice. It has been shown previously that germline gene deletion can result in compensatory

effects, and differences in phenotypes between constitutive knockouts, conditional knockouts, and therapeutic inhibition of gene function can be expected (46). However, it is also possible that inhibition of IL-11–driven fibro-inflammation in *Il11ra1*^{-/-} mice in the first week, when inflammatory effects are strongest (47), has additional anti-inflammatory effects when compared to therapeutic interventions at later time points. It is interesting to note that inhibiting IL-11 down-regulates canonical TGF β /SMAD signaling that is a disease-modifying effect of anti-IL-11 therapy, which we have also seen in models of liver disease (24).

There are limitations to our current study. Histological characterization of IL-11 did not define the cell types secreting IL-11. IL-11 signaling in lung fibroblasts also requires deeper study as while we confirm robust ERK-dependent effects, as we documented in other stromal cells (12, 24), the downstream molecular mechanisms remain to be elucidated. We highlight that genetic or pharmacologic inhibition of IL-11 had no overall effect on survival in the BLM lung fibrosis model, which could reflect biology or relate to the model. Although the BLM model is the best characterized model of lung fibrosis in mice, it has limitations and does not recapitulate some features of IPF pathology, morbidity, or mortality. The particular problem with survival analysis in the BLM model is highlighted by the fact that drugs approved for IPF and with established mortality benefit in patients (5, 48) have no effect on mortality in this model (49), whereas other interventions do (50, 51). BLM administration in mice elicits a strong inflammatory component in the lung not seen in IPF, and interventions that disrupt this phase can afford protection against fibrosis when administered prophylactically in the mouse (33, 52–54). It is also the case that therapies shown to work in the BLM model, such as imatinib (55) and endothelin receptor antagonists (56), have subsequently been ineffective in clinical trials (57–59). Alternative models, such as the humanized SCID mouse model of IPF, can be used, but again, therapies effective in this model have failed in the clinic, such as anti-IL-13 (21, 26). Follow-up studies using cell type–specific, conditional mouse knockouts are needed to clarify further IL-11 effects in the lung.

The antifibrotic drugs pirfenidone and nintedanib are approved for IPF, but it remains a progressive and fatal disease despite drug therapy, which is associated with a number of side effects. Inhibition of IL-11 is not expected to be associated with these or other side effects because it is not expressed at detectable amounts in healthy tissues. Consistent with this, knockout humans or mice do not suffer from infections, cardiovascular disease, or cancer (12, 60, 61), and there is no evidence of genetic selective pressure for loss-of-function variants in IL-11 or its receptor (62). We propose IL-11 as a therapeutically accessible target for pulmonary fibrosis and IPF.

MATERIALS AND METHODS

Study design

In this study, we used ex vivo human and mouse samples and in vivo mouse experiments to study the effects of IL-11 in pulmonary fibrosis. Human tissue specimens were obtained under the auspices of the Cedars-Sinai Medical Center Institutional Review Board–approved protocol (Pro00051481). Animal procedures were performed according to the protocols approved by the SingHealth Institutional Animal Care and Use Committee (IACUC).

Microarray and RNA-seq datasets of lung samples and fibroblasts from patients with IPF and healthy individuals (GSE47460 and

GSE118933) were reanalyzed for *IL11* expression, and IL-11 protein expression was examined in lung tissue and fibroblasts from patients with IPF by immunohistochemistry and ELISA techniques. The effects of IL-11 on fibrosis were examined using gain-of-function approaches both in vitro in primary human lung fibroblast cultures and in vivo by systemic IL-11 administration and in fibroblast-specific *Il11*-expressing transgenic mice. Loss-of-function experiments were performed in *Il11ra1*-deleted fibroblasts treated with various profibrotic factors, and the effects of genetic inhibition of *Il11* in the BLM model of pulmonary fibrosis were explored using *Il11ra1* knockout mice. We developed a neutralizing antibody against IL-11 and used this in primary fibroblast experiments and in therapeutic prevention and reversal studies of pulmonary fibrosis in the BLM mouse model. RNA-seq and Western blot analysis were performed on IL-11– or TGF β 1-treated fibroblasts, as well as on lung samples from BLM-challenged mice treated with anti-IL-11 antibodies.

For in vivo models, experiments were designed to detect 20% differences between treatment groups or genotype-dependent effects at 80% power ($\alpha = 0.05$). Sample size for tissue- and cell-based assays were determined based on sample availability and technical needs.

For BLM experiments, animals were randomly assigned to experimental groups on the day before treatment. Randomization was not applicable to transgenic or knockout mice that were assigned to treatment groups based on their genotypes. For in vivo and in vitro gain- and loss-of-function studies, investigators were not blinded to different treatment groups or genotypes. Histology and pathological scoring of lung tissue samples were performed blinded to treatment and genotypes. Cell culture experiments were replicated independently at least twice per experiment. Outlier tests were performed using the ROUT method (GraphPad Prism). For anti-IL-11 antibody treatment in the BLM model, mice that displayed major respiratory distress or had pronounced weight loss (>20%) before the start of treatment were euthanized according to local IACUC guidelines and excluded from analysis. Mice that displayed these signs during the antibody treatment periods were euthanized and treated as deaths, which are represented in the mortality graphs. Further details are described in Supplementary Materials and Methods.

Statistical analysis

Microarray and RNA-seq data were imported and analyzed in R 3.5.2 and described in detail in Supplementary Materials and Methods. All other analyses were performed using GraphPad Prism software (version 6.07). Statistical analyses were performed using two-sided Student's *t* tests or by one-way ANOVA as indicated in the figure legends. *P* values were corrected for multiple hypothesis testing using either the Benjamini-Hochberg procedure (for comparisons of multiple couples of control and treatment), Dunnett's test (for comparisons between multiple treatments to a single control), or Tukey's test (for comparisons between multiple treatment groups). *P* values <0.05 are regarded as statistically significant.

SUPPLEMENTARY MATERIALS

stm.sciencemag.org/cgi/content/full/11/511/eaaw1237/DC1
Materials and Methods

- Fig. S1. Correlation between the gene expression of IL-6 family cytokines and IL-13 with lung function and fibrotic genes in healthy subjects.
- Fig. S2. IL-11 protein expression is elevated in the lungs of patients with IPF.
- Fig. S3. IL-11 stimulates both human and mouse lung fibroblast activation in vitro.
- Fig. S4. Pharmacologic and transgenic IL-11 gain of function induces fibroblast activation and collagen deposition in the mouse lung.

- Fig. S5. Primary lung fibroblasts from *Il11ra1^{-/-}* mice exhibit intact SMAD signaling but are not able to synthesize profibrotic proteins when stimulated by various profibrotic stimulants.
- Fig. S6. BLM-induced lung fibrosis is attenuated in *Il11ra1^{-/-}* mice.
- Fig. S7. Development of neutralizing anti-IL-11 antibodies.
- Fig. S8. Multiple profibrotic stimulants activate noncanonical IL-11 signaling to induce fibroblast activation.
- Fig. S9. X203 attenuates the fibrotic phenotypes of IPF fibroblasts via ERK signaling pathway inhibition.
- Fig. S10. X203 treatment prevents BLM-induced lung fibrosis.
- Fig. S11. GSEA of RNA-seq data of the transcriptional response to X203 treatment from day 7 in the BLM model.
- Fig. S12. X203 treatment reverses established pulmonary fibrosis.
- Fig. S13. ERK and SMAD2, not STAT3, signaling are reduced in the lungs of X203-treated mice after BLM administration.
- Data file S1. Raw data.
- Data file S2. Uncropped Western blots.
- References (63–84)

REFERENCES AND NOTES

- V. J. Thannickal, G. B. Toews, E. S. White, J. P. Lynch III, F. J. Martinez, Mechanisms of pulmonary fibrosis. *Annu. Rev. Med.* **55**, 395–417 (2004).
- D. J. Lederer, F. J. Martinez, Idiopathic pulmonary fibrosis. *N. Engl. J. Med.* **378**, 1811–1823 (2018).
- Idiopathic Pulmonary Fibrosis Clinical Research Network, G. Raghu, K. J. Anstrom, T. E. King Jr., J. A. Lasky, F. J. Martinez, Prednisone, azathioprine, and N-acetylcysteine for pulmonary fibrosis. *N. Engl. J. Med.* **366**, 1968–1977 (2012).
- Y. Li, D. Jiang, J. Liang, E. B. Meltzer, A. Gray, R. Miura, L. Wogensen, Y. Yamaguchi, P. W. Noble, Severe lung fibrosis requires an invasive fibroblast phenotype regulated by hyaluronan and CD44. *J. Exp. Med.* **208**, 1459–1471 (2011).
- L. Richeldi, R. M. du Bois, G. Raghu, A. Azuma, K. K. Brown, U. Costabel, V. Cottin, K. R. Flaherty, D. M. Hansell, Y. Inoue, D. S. Kim, M. Kolb, A. G. Nicholson, P. W. Noble, M. Selman, H. Taniguchi, M. Brun, F. Le Mauff, M. Girard, S. Stowasser, R. Schlenker-Herceg, B. Disse, H. R. Collard, Efficacy and safety of nintedanib in idiopathic pulmonary fibrosis. *N. Engl. J. Med.* **370**, 2071–2082 (2014).
- T. E. King Jr., W. Z. Bradford, S. Castro-Bernardini, E. A. Fagan, I. Glaspole, M. K. Glassberg, E. Gorina, P. M. Hopkins, D. Kardatzke, L. Lancaster, D. J. Lederer, S. D. Nathan, C. A. Pereira, S. A. Sahn, R. Sussman, J. J. Swigris, P. W. Noble, A phase 3 trial of pirfenidone in patients with idiopathic pulmonary fibrosis. *N. Engl. J. Med.* **370**, 2083–2092 (2014).
- A. L. Mora, M. Rojas, A. Pardo, M. Selman, Emerging therapies for idiopathic pulmonary fibrosis, a progressive age-related disease. *Nat. Rev. Drug Discov.* **16**, 755–772 (2017).
- I. E. Fernandez, O. Eickelberg, The impact of TGF- β on lung fibrosis. *Proc. Am. Thorac. Soc.* **9**, 111–116 (2012).
- D. G. Morris, X. Huang, N. Kaminski, Y. Wang, S. D. Shapiro, G. Dolganov, A. Glick, D. Sheppard, Loss of integrin $\alpha v\beta 6$ -mediated TGF- β activation causes Mmp12-dependent emphysema. *Nature* **422**, 169–173 (2003).
- P. Aluwihare, Z. Mu, Z. Zhao, D. Yu, P. H. Weinreb, G. S. Horan, S. M. Violette, J. S. Munger, Mice that lack activity of alphavbeta6- and alphavbeta8-integrins reproduce the abnormalities of Tgfb1- and Tgfb3-null mice. *J. Cell Sci.* **122**, 227–232 (2009).
- J. S. Munger, X. Huang, H. Kawakatsu, M. J. Griffiths, S. L. Dalton, J. Wu, J. F. Pittet, N. Kaminski, C. Garat, M. A. Matthay, D. B. Rifkin, D. Sheppard, The integrin alpha v beta 6 binds and activates latent TGF beta 1: A mechanism for regulating pulmonary inflammation and fibrosis. *Cell* **96**, 319–328 (1999).
- S. Schafer, S. Viswanathan, A. A. Widjaja, W.-W. Lim, A. Moreno-Moral, D. M. DeLaughter, B. Ng, G. Patone, K. Chow, E. Khin, J. Tan, S. P. Chothani, L. Ye, O. J. L. Rackham, N. S. J. Ko, N. E. Sahib, C. J. Pua, N. T. G. Zhen, C. Xie, M. Wang, H. Maatz, S. Lim, K. Saar, S. Blachut, E. Petretto, S. Schmidt, T. Putoczki, N. Guimaraes-Camboa, H. Wakimoto, S. van Heesch, K. Sigmundsson, S. L. Lim, J. L. Soon, V. T. T. Chao, Y. L. Chua, T. E. Tan, S. M. Evans, Y. J. Loh, M. H. Jamal, K. K. Ong, K. C. Chua, B.-H. Ong, M. J. Chakraramakkil, J. G. Seidman, C. E. Seidman, N. Hubner, K. Y. K. Sin, S. A. Cook, IL-11 is a crucial determinant of cardiovascular fibrosis. *Nature* **552**, 110–115 (2017).
- G. E. Lindahl, C. J. Stock, X. Shi-Wen, P. Leoni, P. Sestini, S. L. Howat, G. Bou-Gharios, A. G. Nicholson, C. P. Denton, J. C. Grutters, T. M. Maher, A. U. Wells, D. J. Abraham, E. A. Renzoni, Microarray profiling reveals suppressed interferon stimulated gene program in fibroblasts from scleroderma-associated interstitial lung disease. *Respir. Res.* **14**, 80 (2013).
- W. Tang, G. P. Geba, T. Zheng, P. Ray, R. J. Homer, C. Kuhn III, R. A. Flavell, J. A. Elias, Targeted expression of IL-11 in the murine airway causes lymphocytic inflammation, bronchial remodeling, and airways obstruction. *J. Clin. Invest.* **98**, 2845–2853 (1996).
- A. B. Waxman, O. Einarsson, T. Seres, R. G. Knickelbein, R. Homer, J. B. Warshaw, R. Johnston, J. A. Elias, Targeted lung expression of interleukin-11 enhances murine tolerance of 100% oxygen and diminishes hyperoxia-induced DNA fragmentation. *J. Clin. Invest.* **101**, 1970–1982 (1998).
- T. Zheng, Z. Zhu, J. Wang, R. J. Homer, J. A. Elias, IL-11: Insights in asthma from overexpression transgenic modeling. *J. Allergy Clin. Immunol.* **108**, 489–496 (2001).
- B. C. Sheridan, C. A. Dinarello, D. R. Meldrum, D. A. Fullerton, C. H. Selzman, R. C. McIntyre Jr., Interleukin-11 attenuates pulmonary inflammation and vasomotor dysfunction in endotoxin-induced lung injury. *Am. J. Physiol.* **277**, L861–L867 (1999).
- L. Richeldi, H. R. Collard, M. G. Jones, Idiopathic pulmonary fibrosis. *Lancet* **389**, 1941–1952 (2017).
- B. Ley, H. R. Collard, T. E. King Jr., Clinical course and prediction of survival in idiopathic pulmonary fibrosis. *Am. J. Respir. Crit. Care Med.* **183**, 431–440 (2011).
- Y. Bauer, J. Tedrow, S. de Bernard, M. Birker-Robaczewska, K. F. Gibson, B. J. Guardela, P. Hess, A. Klenk, K. O. Lindell, S. Poirey, B. Renault, M. Rey, E. Weber, O. Nayler, N. Kaminski, A novel genomic signature with translational significance for human idiopathic pulmonary fibrosis. *Am. J. Respir. Cell Mol. Biol.* **52**, 217–231 (2015).
- J. M. Parker, I. N. Glaspole, L. H. Lancaster, T. J. Haddad, D. She, S. L. Roseti, J. P. Fiening, E. P. Grant, C. M. Kell, K. R. Flaherty, A Phase 2 randomized controlled study of tralokinumab in subjects with idiopathic pulmonary fibrosis. *Am. J. Respir. Crit. Care Med.* **197**, 94–103 (2018).
- Y. Geng, X. Liu, J. Liang, D. M. Habiels, K. Vrishika, A. L. Coelho, N. Deng, T. Xie, Y. Wang, N. Liu, G. Huang, A. Kurkciyan, Z. Liu, J. Tang, C. M. Hogaboam, D. Jiang, P. W. Noble, PD-L1 on invasive fibroblasts drives fibrosis in a humanized model of idiopathic pulmonary fibrosis. *JCI Insight* **4**, 125326 (2019).
- Y. Yata, DNase I-hypersensitive sites enhance $\alpha 1(I)$ collagen gene expression in hepatic stellate cells. *Hepatology* **37**, 267–276 (2003).
- A. A. Widjaja, B. K. Singh, E. Adami, S. Viswanathan, J. Dong, G. A. D'Agostino, B. Ng, W. W. Lim, J. Tan, B. S. Paleja, M. Tripathi, S. Y. Lim, S. G. Shekeran, S. P. Chothani, A. Rabes, M. Sombetzki, E. Bruunstroem, L. P. Min, R. A. Sinha, S. Albani, P. M. Yen, S. Schafer, S. A. Cook, Inhibiting interleukin 11 signaling reduces hepatocyte death and liver fibrosis, inflammation, and steatosis in mouse models of non-alcoholic steatohepatitis. *Gastroenterology* **157**, 777–792.e14 (2019).
- D. Saleh, K. Furukawa, M. S. Tsao, A. Maghazachi, B. Corrin, M. Yanagisawa, P. J. Barnes, A. Giard, Elevated expression of endothelin-1 and endothelin-converting enzyme-1 in idiopathic pulmonary fibrosis: Possible involvement of proinflammatory cytokines. *Am. J. Respir. Cell Mol. Biol.* **16**, 187–193 (1997).
- L. A. Murray, H. Zhang, S. R. Oak, A. L. Coelho, A. Herath, K. R. Flaherty, J. Lee, M. Bell, D. A. Knight, F. J. Martinez, M. A. Sleeman, E. L. Herzog, C. M. Hogaboam, Targeting interleukin-13 with tralokinumab attenuates lung fibrosis and epithelial damage in a humanized SCID idiopathic pulmonary fibrosis model. *Am. J. Respir. Cell Mol. Biol.* **50**, 985–994 (2014).
- H. N. Antoniades, M. A. Bravo, R. E. Avila, T. Galanopoulos, J. Neville-Golden, M. Maxwell, M. Selman, Platelet-derived growth factor in idiopathic pulmonary fibrosis. *J. Clin. Invest.* **86**, 1055–1064 (1990).
- A. Mozaffarian, A. W. Brewer, E. S. Trueblood, I. G. Luzina, N. W. Todd, S. P. Atamas, H. A. Arnett, Mechanisms of oncostatin M-induced pulmonary inflammation and fibrosis. *J. Immunol.* **181**, 7243–7253 (2008).
- T. E. King Jr., A. Pardo, M. Selman, Idiopathic pulmonary fibrosis. *Lancet* **378**, 1949–1961 (2011).
- I. Y. Adamson, D. H. Bowden, The pathogenesis of bleomycin-induced pulmonary fibrosis in mice. *Am. J. Pathol.* **77**, 185–197 (1974).
- R. G. Jenkins, B. B. Moore, R. C. Chambers, O. Eickelberg, M. Königshoff, M. Kolb, G. J. Laurent, C. B. Nanthakumar, M. A. Olman, A. Pardo, An official American Thoracic Society workshop report: Use of animal models for the preclinical assessment of potential therapies for pulmonary fibrosis. *Am. J. Respir. Cell Mol. Biol.* **56**, 667–679 (2017).
- M. Selman, V. Ruiz, S. Cabrera, L. Segura, R. Ramírez, R. Barrios, A. Pardo, TIMP-1, -2, -3, and -4 in idiopathic pulmonary fibrosis. A prevailing nondegradative lung microenvironment? *Am. J. Physiol. Lung Cell. Mol. Physiol.* **279**, L562–L574 (2000).
- B. B. Moore, W. E. Lawson, T. D. Oury, T. H. Sisson, K. Raghavendran, C. M. Hogaboam, Animal models of fibrotic lung disease. *Am. J. Respir. Cell Mol. Biol.* **49**, 167–179 (2013).
- Z. Yang, Z. Mu, B. Dabovic, V. Jurukovski, D. Yu, J. Sung, X. Xiong, J. S. Munger, Absence of integrin-mediated TGFbeta1 activation in vivo recapitulates the phenotype of TGFbeta1-null mice. *J. Cell Biol.* **176**, 787–793 (2007).
- R. Kimura, M. Maeda, A. Arita, Y. Oshima, M. Obana, T. Ito, Y. Yamamoto, T. Mohri, T. Kishimoto, I. Kawase, Y. Fujio, J. Azuma, Identification of cardiac myocytes as the target of interleukin 11, a cardioprotective cytokine. *Cytokine* **38**, 107–115 (2007).
- M. Obana, M. Maeda, K. Takeda, A. Hayama, T. Mohri, T. Yamashita, Y. Nakao, I. Komuro, K. Takeda, G. Matsumiya, J. Azuma, Y. Fujio, Therapeutic activation of signal transducer and activator of transcription 3 by interleukin-11 ameliorates cardiac fibrosis after myocardial infarction. *Circulation* **121**, 684–691 (2010).
- M. Zhu, B. Lu, Q. Cao, Z. Wu, Z. Xu, W. Li, X. Yao, F. Liu, IL-11 attenuates liver ischemia/reperfusion injury (IRI) through STAT3 signaling pathway in mice. *PLOS ONE* **10**, e0126296 (2015).

38. W. L. Trepicchio, M. Bozza, P. Bouchard, A. J. Dorner, Protective effect of rhIL-11 in a murine model of acetaminophen-induced hepatotoxicity. *Toxicol. Pathol.* **29**, 242–249 (2016).
39. M. Stangou, G. Bhagyal, P.-C. Lai, J. Smith, J. C. Keith Jr., J. J. Boyle, C. D. Pusey, T. Cook, F. W. K. Tam, Effect of IL-11 on glomerular expression of TGF-beta and extracellular matrix in nephrotoxic nephritis in Wistar Kyoto rats. *J. Nephrol.* **24**, 106–111 (2011).
40. H. T. Lee, S. W. Park, M. Kim, A. Ham, L. J. Anderson, K. M. Brown, V. D. D'Agati, G. N. Cox, Interleukin-11 protects against renal ischemia and reperfusion injury. *Am. J. Physiol. Renal Physiol.* **303**, F1216–F1224 (2012).
41. M. Boerma, J. Wang, A. F. Burnett, A. D. Santin, J. J. Roman, M. Hauer-Jensen, Local administration of interleukin-11 ameliorates intestinal radiation injury in rats. *Cancer Res.* **67**, 9501–9506 (2007).
42. B. Greenwood-Van Meerveld, K. Tyler, J. C. Keith Jr., Recombinant human interleukin-11 modulates ion transport and mucosal inflammation in the small intestine and colon. *Lab. Invest.* **80**, 1269–1280 (2000).
43. Q. Chen, L. Rabach, P. Noble, T. Zheng, C. G. Lee, R. J. Homer, J. A. Elias, IL-11 receptor α in the pathogenesis of IL-13-induced inflammation and remodeling. *J. Immunol.* **174**, 2305–2313 (2005).
44. Y. P. Moodley, A. K. Scaffidi, N. L. Misso, C. Keerthisingam, R. J. McAnulty, G. J. Laurent, S. E. Mutsaers, P. J. Thompson, D. A. Knight, Fibroblasts isolated from normal lungs and those with idiopathic pulmonary fibrosis differ in interleukin-6/gp130-mediated cell signaling and proliferation. *Am. J. Pathol.* **163**, 345–354 (2003).
45. A. Strikoudis, A. Cieślak, L. Offredo, Y.-W. Chen, N. Patel, A. Saqi, D. J. Lederer, H.-W. Snoeck, Modeling of fibrotic lung disease using 3D organoids derived from human pluripotent stem cells. *Cell Rep.* **27**, 3709–3723.e5 (2019).
46. A. Rossi, Z. Kontarakis, C. Gerri, H. Nolte, S. Höller, M. Krüger, D. Y. R. Stainier, Genetic compensation induced by deleterious mutations but not gene knockdowns. *Nature* **524**, 230–233 (2015).
47. N. I. Chaudhary, A. Schnapp, J. E. Park, Pharmacologic differentiation of inflammation and fibrosis in the rat bleomycin model. *Am. J. Respir. Crit. Care Med.* **173**, 769–776 (2006).
48. S. D. Nathan, C. Albera, W. Z. Bradford, U. Costabel, I. Glaspole, M. K. Glassberg, D. R. Kardatzke, M. Daigl, K.-U. Kirchgaessler, L. H. Lancaster, D. J. Lederer, C. A. Pereira, J. J. Swigris, D. Valeye, P. W. Noble, Effect of pirfenidone on mortality: Pooled analyses and meta-analyses of clinical trials in idiopathic pulmonary fibrosis. *Lancet Respir. Med.* **5**, 33–41 (2017).
49. G. Yu, A. Tzouvelekis, R. Wang, J. D. Herazo-Maya, G. H. Ibarra, A. Srivastava, J. P. W. de Castro, G. Delulii, F. Ahangari, T. Woolard, N. Aurelien, R. Arrojo, E. Drigo, Y. Gan, M. Graham, X. Liu, R. J. Homer, T. S. Scanlan, P. Mannam, P. J. Lee, E. L. Herzog, A. C. Bianco, N. Kaminski, Thyroid hormone inhibits lung fibrosis in mice by improving epithelial mitochondrial function. *Nat. Med.* **24**, 39–49 (2018).
50. M. Inayama, Y. Nishioka, M. Azuma, S. Muto, Y. Aono, H. Makino, K. Tani, H. Uehara, K. Izumi, A. Itai, S. Sone, A novel I κ B kinase- β inhibitor ameliorates bleomycin-induced pulmonary fibrosis in mice. *Am. J. Respir. Crit. Care Med.* **173**, 1016–1022 (2006).
51. S. Murakami, N. Nagaya, T. Itoh, M. Kataoka, T. Iwase, T. Horio, Y. Miyahara, Y. Sakai, K. Kawaga, H. Kimura, Prostacyclin agonist with thromboxane synthase inhibitory activity (ONO-1301) attenuates bleomycin-induced pulmonary fibrosis in mice. *Am. J. Physiol. Lung Cell. Mol. Physiol.* **290**, L59–L65 (2006).
52. L. Wollin, I. Maillet, V. Quesniaux, A. Holweg, B. Ryffel, Antifibrotic and anti-inflammatory activity of the tyrosine kinase inhibitor nintedanib in experimental models of lung fibrosis. *J. Pharmacol. Exp. Ther.* **349**, 209–220 (2014).
53. H. Oku, T. Shimizu, T. Kawabata, M. Nagira, I. Hikita, A. Ueyama, S. Matsushima, M. Torii, A. Arimura, Antifibrotic action of pirfenidone and prednisolone: Different effects on pulmonary cytokines and growth factors in bleomycin-induced murine pulmonary fibrosis. *Eur. J. Pharmacol.* **590**, 400–408 (2008).
54. T. Takugawa, H. Mukae, T. Hayashi, H. Ishii, K. Abe, T. Fujii, H. Oku, M. Miyazaki, J. Kadota, S. Kohno, Pirfenidone attenuates expression of HSP47 in murine bleomycin-induced pulmonary fibrosis. *Eur. Respir. J.* **24**, 57–65 (2004).
55. Y. Aono, Y. Nishioka, M. Inayama, M. Ugai, J. Kishi, H. Uehara, K. Izumi, S. Sone, Imatinib as a novel antifibrotic agent in bleomycin-induced pulmonary fibrosis in mice. *Am. J. Respir. Crit. Care Med.* **171**, 1279–1285 (2005).
56. S. H. Park, D. Saleh, A. Giaid, R. P. Michel, Increased endothelin-1 in bleomycin-induced pulmonary fibrosis and the effect of an endothelin receptor antagonist. *Am. J. Respir. Crit. Care Med.* **156**, 600–608 (1997).
57. C. E. Daniels, J. A. Lasky, A. H. Limper, K. Mieras, E. Gabor, D. R. Schroeder, Imatinib treatment for idiopathic pulmonary fibrosis. *Am. J. Respir. Crit. Care Med.* **181**, 604–610 (2010).
58. T. E. King Jr., K. K. Brown, G. Raghu, R. M. du Bois, D. A. Lynch, F. Martinez, D. Valeye, I. Leconte, A. Morganti, S. Roux, J. Behr, BUILD-3: A randomized, controlled trial of bosentan in idiopathic pulmonary fibrosis. *Am. J. Respir. Crit. Care Med.* **184**, 92–99 (2011).
59. G. Raghu, R. Million-Rousseau, A. Morganti, L. Perchenet, J. Behr; MUSIC Study Group, Macitentan for the treatment of idiopathic pulmonary fibrosis: The randomised controlled MUSIC trial. *Eur. Respir. J.* **42**, 1622–1632 (2013).
60. H. H. Nandurkar, L. Robb, D. Tarlinton, L. Barnett, F. Köntgen, C. G. Begley, Adult mice with targeted mutation of the interleukin-11 receptor (IL11Ra) display normal hematopoiesis. *Blood* **90**, 2148–2159 (1997).
61. E. Brischoux-Boucher, A. Trimouille, G. Baujat, A. Goldenberg, E. Schaefer, B. Guichard, P. Hannequin, G. Paternoster, S. Baer, C. Cabrol, E. Weber, G. Godfrin, M. Lenoir, D. Lacombe, C. Collet, L. Van Maldergem, IL11RA-related Crouzon-like autosomal recessive craniosynostosis in 10 new patients: Resemblances and differences. *Clin. Genet.* **94**, 373–380 (2018).
62. M. Lek, K. J. Karczewski, E. V. Minikel, K. E. Samocha, E. Banks, T. Fennell, A. H. O'Donnell-Luria, J. S. Ware, A. J. Hill, B. B. Cummings, T. Tukiainen, D. P. Birnbaum, J. A. Kosmicki, L. E. Duncan, K. Estrada, F. Zhao, J. Zou, E. Pierce-Hoffman, J. Berghou, D. N. Cooper, N. Deflaux, M. DePristo, R. Do, J. Flannick, M. Fromer, L. Gauthier, J. Goldstein, N. Gupta, D. Howrigan, K. Iezzoni, M. I. Kurki, A. L. Moonshine, P. Natarajan, L. Orozco, G. M. Peloso, R. Poplin, M. A. Rivas, V. Ruano-Rubio, S. A. Rose, D. M. Ruderfer, K. Shakir, P. D. Stenson, C. Stevens, B. P. Thomas, G. Tiao, M. T. Tusie-Luna, B. Weisburd, H.-H. Won, D. Yu, D. M. Altshuler, D. Ardissino, M. Boehnke, J. Danesh, S. Donnelly, R. Elosua, J. C. Florez, S. B. Gabriel, G. Getz, S. J. Glatt, C. M. Hultman, S. Kathiresan, M. Laakso, S. McCarroll, M. I. McCarthy, D. McGovern, R. McPherson, B. M. Neale, A. Palotie, S. M. Purcell, D. Saleheen, J. M. Schatz, P. Sklar, P. F. Sullivan, J. Tuomilehto, M. T. Tsuang, H. C. Watkins, J. G. Wilson, M. J. Daly, D. G. MacArthur; Exome Aggregation Consortium, Analysis of protein-coding genetic variation in 60,706 humans. *Nature* **536**, 285–291 (2016).
63. G. K. Smyth, Linear models and empirical Bayes methods for assessing differential expression in microarray experiments. *Stat. Appl. Genet. Mol. Biol.* **3**, Article3 (2004).
64. M. E. Ritchie, B. Phipson, D. Wu, Y. Hu, C. W. Law, W. Shi, G. K. Smyth, limma powers differential expression analyses for RNA-sequencing and microarray studies. *Nucleic Acids Res.* **43**, e47 (2015).
65. J. Gross, U. Ligges, nortest: Tests for Normality, *R package version 1* (2015).
66. J. Wang, R. Zamar, A. Marazzi, V. Yohai, M. Salibian-Barrera, R. Maronna, E. Zivot, D. Rocke, D. Martin, M. Maechler, Others, robust: Port of the S+ "Robust Library". *R package version 0.4–18* (2017).
67. A. Canty, B. Ripley, Others, boot: Bootstrap R (S-Plus) functions, *R package version 1* (2012).
68. A. C. Davison, D. V. Hinkley, *Bootstrap Methods and Their Application* (Cambridge Univ. Press, 1997).
69. M. Hervé, RVAideMemoire: Testing and plotting procedures for biostatistics, *R package version 0.9–68* (2017).
70. A. K. Lovgren, J. J. Kovacs, T. Xie, E. N. Potts, Y. Li, W. M. Foster, J. Liang, E. B. Meltzer, D. Jiang, R. J. Lefkowitz, P. W. Noble, β -Arrestin deficiency protects against pulmonary fibrosis in mice and prevents fibroblast invasion of extracellular matrix. *Sci. Transl. Med.* **3**, 74ra23 (2011).
71. T. Xie, J. Liang, N. Liu, C. Huan, Y. Zhang, W. Liu, M. Kumar, R. Xiao, J. D'Armiento, D. Metzger, P. Chambon, V. E. Papaioannou, B. R. Stripp, D. Jiang, P. W. Noble, Transcription factor TBX4 regulates myofibroblast accumulation and lung fibrosis. *J. Clin. Invest.* **126**, 3626 (2016).
72. A. M. Bolger, M. Lohse, B. Usadel, Trimmomatic: A flexible trimmer for Illumina sequence data. *Bioinformatics* **30**, 2114–2120 (2014).
73. A. Dobin, C. A. Davis, F. Schlesinger, J. Drenkow, C. Zaleski, S. Jha, P. Batut, M. Chaisson, T. R. Gingeras, STAR: Ultrafast universal RNA-seq aligner. *Bioinformatics* **29**, 15–21 (2013).
74. Y. Liao, G. K. Smyth, W. Shi, The Subread aligner: Fast, accurate and scalable read mapping by seed-and-vote. *Nucleic Acids Res.* **41**, e108 (2013).
75. M. I. Love, W. Huber, S. Anders, Moderated estimation of fold change and dispersion for RNA-seq data with DESeq2. *Genome Biol.* **15**, 550 (2014).
76. B. Klaus, K. Strimmer, fdrtool: Estimation of (local) false discovery rates and higher criticism, *R package version 3* (2013); <http://CRAN.R-project.org/package=fdrtool>.
77. A. Sergushichev, An algorithm for fast preranked gene set enrichment analysis using cumulative statistic calculation. *bioRxiv* (2016).
78. S. Durinck, Y. Moreau, A. Kasprzyk, S. Davis, B. De Moor, A. Brazma, W. Huber, BioMart and Bioconductor: A powerful link between biological databases and microarray data analysis. *Bioinformatics* **21**, 3439–3440 (2005).
79. S. Durinck, P. T. Spellman, E. Birney, W. Huber, Mapping identifiers for the integration of genomic datasets with the R/Bioconductor package biomaRt. *Nat. Protoc.* **4**, 1184–1191 (2009).
80. R. Kolde, pheatmap: Pretty Heatmaps, *R package version 1.0.8* (2015).
81. B. Zheng, Z. Zhang, C. M. Black, B. de Crombrugghe, C. P. Denton, Ligand-dependent genetic recombination in fibroblasts: A potentially powerful technique for investigating gene function in fibrosis. *Am. J. Pathol.* **160**, 1609–1617 (2002).
82. T. Ashcroft, J. M. Simpson, V. Timbrell, Simple method of estimating severity of pulmonary fibrosis on a numerical scale. *J. Clin. Pathol.* **41**, 467–470 (1988).

83. B. Johnsson, S. Löfås, G. Lindquist, Immobilization of proteins to a carboxymethylated modified gold surface for biospecific interaction analysis in surface plasmon resonance sensors. *Anal. Biochem.* **198**, 268–277 (1991).
84. T. Fei, K. Xia, Z. Li, B. Zhou, S. Zhu, H. Chen, J. Zhang, Z. Chen, H. Xiao, J.-D. Han, Y.-G. Chen, Genome-wide mapping of SMAD target genes reveals the role of BMP signaling in embryonic stem cell fate determination. *Genome Res.* **20**, 36–44 (2010).

Acknowledgments: We acknowledge B. L. George, E. Khin, N. E. Sahib, M. Wang, S.-Y. Lim, P.-M. Lio, B.-Y. Soh, and E. Petretto for their technical expertise and support. **Funding:** The research was supported by the National Medical Research Council (NMRC) Singapore STaR awards to S.A.C. (NMRC/STaR/0011/2012 and NMRC/STaR/0029/2017), the NMRC Centre Grant to the NHCS, Goh Foundation, Tanoto Foundation, and a grant from the Fondation Leducq. T.M.M. was supported by an NIH Clinician Scientist Fellowship (NIHR ref. CS-2013-13-017) and a British Lung Foundation Chair in Respiratory Research (C17-3). A.A.W. was supported by NMRC Singapore (NMRC/OFYIRG/0053/2017). **Author contributions:** B.N., S.S., and S.A.C. conceived and designed the study. B.N., J.D., S.V., A.A.W., J.T., and B.H. performed in vitro cell culture, cell biology, and molecular biology experiments. B.N., J.D., A.A.W., N.S.J.K., and J.T. performed in vivo gain- and loss-of-function mouse studies. C.J.P. performed RNA-seq experiments. N.G.-C. and S.M.E. performed gain-of-function studies on *Col1a1-GFP* mice. B.N., W.-W.L., and C.X. performed histology analysis. A.-M.C. analyzed pharmacokinetics and biodistribution studies. S.V. and A.A.W. performed in vitro antibody screening. G.D. performed computational analysis. A.J.B., T.M.M., J.L., D.J., and P.W.N. provided critical reagents for the study. B.N., J.D., S.V., G.D., A.A.W.,

S.P.C., S.S., and S.A.C. analyzed the data. B.N., G.D., S.S., and S.A.C. prepared the manuscript with input from co-authors. **Competing interests:** S.A.C. and S.S. are co-inventors of the patent applications (WO/2017/103108: TREATMENT OF FIBROSIS, WO/2018/109174: IL-11 ANTIBODIES, WO/2018/109170: IL-11RA ANTIBODIES). S.A.C. and S.S. are co-founders and shareholders of Enleofen Bio Pte Ltd, a company that develops anti-IL-11 therapeutics. **Data and materials availability:** RNA-seq and microarray data reanalyzed in the paper are in publicly available libraries from GEO under accession nos. GSE118933 and GSE47460 and www.lung-genomics.org/. Sequencing data generated for this study can be downloaded from the GEO repository GSE130983. R code used for microarray and RNA-seq analyses is available at https://github.com/gdagstn/IL11_Lung. Primary data are made available in table S13 in data file S1. All data associated with this study are present in the paper or the Supplementary Materials.

Submitted 21 November 2018

Resubmitted 7 March 2019

Accepted 11 August 2019

Published 25 September 2019

10.1126/scitranslmed.aaw1237

Citation: B. Ng, J. Dong, G. D'Agostino, S. Viswanathan, A. A. Widjaja, W.-W. Lim, N. S. J. Ko, J. Tan, S. P. Chothani, B. Huang, C. Xie, C. J. Pua, A.-M. Chacko, N. Guimaraes-Camboa, S. M. Evans, A. J. Byrne, T. M. Maher, J. Liang, D. Jiang, P. W. Noble, S. Schafer, S. A. Cook, Interleukin-11 is a therapeutic target in idiopathic pulmonary fibrosis. *Sci. Transl. Med.* **11**, eaaw1237 (2019).

Science Translational Medicine

Interleukin-11 is a therapeutic target in idiopathic pulmonary fibrosis

Benjamin Ng, Jinrui Dong, Giuseppe D'Agostino, Sivakumar Viswanathan, Anissa A. Widjaja, Wei-Wen Lim, Nicole S. J. Ko, Jessie Tan, Sonia P. Chothoni, Benjamin Huang, Chen Xie, Chee Jian Pua, Ann-Marie Chacko, Nuno Guimaraes-Camboa, Sylvia M. Evans, Adam J. Byrne, Toby M. Maher, Jiurong Liang, Dianhua Jiang, Paul W. Noble, Sebastian Schafer and Stuart A. Cook

Sci Transl Med 11, eaaw1237.
DOI: 10.1126/scitranslmed.aaw1237

Targeting IL-11 in lung fibrosis

In idiopathic pulmonary fibrosis (IPF), chronic activation of invasive fibroblasts is responsible for fibrotic scar formation in the lungs. Patients with IPF present progressive difficulty to breathe, pulmonary hypertension, and respiratory failure. The pathophysiological mechanisms remain unclear. Interleukin-11 (IL-11) has been shown to participate in kidney and cardiac fibrosis. However, conflicting data suggest that IL-11 can either be pro- or antifibrotic. Now, Ng *et al.* reported that in patients with IPF, IL-11 was up-regulated in invasive lung fibroblasts. In vitro and in vivo experiments demonstrated that IL-11 exerted profibrotic effects by driving fibroblast activation. Targeting IL-11 with a neutralizing antibody had therapeutic effects in a mouse model of established pulmonary fibrosis.

ARTICLE TOOLS

<http://stm.sciencemag.org/content/11/511/eaaw1237>

SUPPLEMENTARY MATERIALS

<http://stm.sciencemag.org/content/suppl/2019/09/23/11.511.eaaw1237.DC1>

RELATED CONTENT

<http://stm.sciencemag.org/content/scitransmed/6/240/240ra76.full>
<http://stm.sciencemag.org/content/scitransmed/10/460/ear8356.full>
<http://stm.sciencemag.org/content/scitransmed/9/384/eaaf4696.full>
<http://stm.sciencemag.org/content/scitransmed/10/426/eaan5174.full>

REFERENCES

This article cites 76 articles, 14 of which you can access for free
<http://stm.sciencemag.org/content/11/511/eaaw1237#BIBL>

PERMISSIONS

<http://www.sciencemag.org/help/reprints-and-permissions>

Use of this article is subject to the [Terms of Service](#)

Science Translational Medicine (ISSN 1946-6242) is published by the American Association for the Advancement of Science, 1200 New York Avenue NW, Washington, DC 20005. 2017 © The Authors, some rights reserved; exclusive licensee American Association for the Advancement of Science. No claim to original U.S. Government Works. The title *Science Translational Medicine* is a registered trademark of AAAS.